

Cite this: *Mater. Horiz.*, 2025,  
12, 10390Received 20th July 2025,  
Accepted 1st September 2025

DOI: 10.1039/d5mh01385b

rsc.li/materials-horizons

## Simultaneous reinforcement and toughening methods and mechanisms of thermosets: a review

Shenao Xue,<sup>ab</sup> Zhen Yu,<sup>b</sup> Zhaobin Tang<sup>b</sup> and Yanlin Liu<sup>id</sup>\*<sup>b</sup>

Thermosets are widely used in aerospace, wind energy, hydrogen storage and semiconductors, etc. The highly crosslinked three-dimensional network structure leads to low impact resistance and poor toughness, however, traditional toughening methods are often accompanied by a reduction in strength, so it is particularly important to achieve a balance between resin strength and toughness. This work reviews the methods and mechanisms of synchronous reinforcement and toughening of commonly used thermosets, including the addition of second-phase modifiers such as thermoplastic polymers, block copolymers, liquid crystal polymers, siloxanes, nanoparticles, etc., as well as changing the network structure by introducing hyperbranched polymers, constructing topological network structures, and introducing sacrificial bonds. Finally, the future directions and challenges of high-performance thermosets are summarized and proposed. Overall, this review provides a comprehensive overview of the latest developments in the methods and mechanisms of synchronous reinforcement and toughening of thermosets, providing guidance for their applications in various high-tech, sustainable, and emerging fields.

### Wider impact

The highly cross-linked structure of thermosets leads to poor toughness, and the toughening process is usually accompanied by a reduction in strength; how to achieve a balance between strength and toughness has received extensive attention in recent years. In a typical thermoset resin system, the phase structure as well as the three-dimensional network structure of the material have a significant effect on the mechanical properties. Therefore, this review summarizes the latest advances in synchronous reinforcement and toughening methods and mechanisms of thermosets, aiming to gain a deeper understanding of their structure–property relationship and guide the construction of high-strength and high-toughness thermosetting resin systems. Specifically, this review categorizes and describes the synchronous reinforcement and toughening methods and mechanisms of thermosets, including the addition of second-phase modifiers, and the modification of network structures. Furthermore, the development prospects and challenges of high-performance thermosets are also discussed. It is expected that this review will provide valuable guidance for the design of high-performance, especially high-strength and high-toughness thermosetting resin materials.

<sup>a</sup> School of Materials Science & Chemical Engineering, Ningbo University, Ningbo 315211, P. R. China

<sup>b</sup> Key Laboratory of Bio-based Polymeric Materials Technology and Application of Zhejiang Province, Laboratory of Polymers and Composites, Ningbo Institute of Materials Technology and Engineering, Chinese Academy of Sciences, Ningbo 315201, P. R. China. E-mail: liuyanlin@nimte.ac.cn



Shenao Xue

Shenao Xue obtained her Bachelor's degree in Materials Science and Engineering from Linyi University in 2023. She is currently pursuing a Master's degree in Materials Engineering at the School of Integration of Science, Education, and Innovation, Ningbo University. Her research is primarily focused on the toughening of epoxy resins.



Zhen Yu

Zhen Yu received a Doctor of Engineering from the Lanzhou Institute of Chemical Physics, Chinese Academy of Sciences in 2025. He is currently conducting postdoctoral research at the Ningbo Institute of Materials Technology and Engineering, Chinese Academy of Sciences. His research focuses on the exploration of novel dynamic chemistry and the study of high-performance, high-efficiency-recycling polymer materials.



# 1 Introduction

Thermosets are essential raw materials utilized across various industries, including plastics, coatings, adhesives, and composites.<sup>1–3</sup> The global resin market was valued at over \$500 billion in 2023, with China being the leading resin producer, contributing more than 40% of global production capacity. Despite these advantages, the highly crosslinked, three-dimensional network structure of thermosets limits their plastic deformation capacity. Furthermore, the internal stresses induced by volume shrinkage during curing further hinder their ability to resist crack initiation and propagation. These limitations constrain the use of thermosets in applications requiring high mechanical strength and toughness, such as in aerospace and electronic packaging.

To address the toughness limitations of thermosets, researchers have explored various toughening strategies, including the incorporation of toughening agents such as rubbers, thermoplastics, and liquid crystal polymers, as well as the modification of monomer and resin network structures. Among these approaches, rubbers, with their low glass transition temperature, can compromise the thermal stability. The inclusion of amorphous thermoplastics, on the other hand, can increase viscosity, negatively affecting processability. The use of liquid crystal polymers presents challenges related to achieving uniform dispersion within the resin matrix, along with high costs and complex molding processes, which limit their broader application. Moreover, the incorporation of grafting modifiers often results in phase separation due to compatibility issues, leading to interface defects.<sup>4</sup> When subjected to external forces, the second-phase particles at these interfaces experience considerable stress, thereby reducing the mechanical strength of the resin. These findings underscore the trade-off between improving toughness and maintaining resin strength, which limits the practical applications of thermosets. Consequently, the development of technologies that simultaneously enhance

both strength and toughness is of paramount importance. However, for thermosetting plastics, achieving maximum elongation and ductility without sacrificing mechanical strength remains a formidable challenge.

To achieve a balance between strength and toughness, researchers have built upon previous methods through various improvements and explorations. Studies have shown that decreasing particle size enhances the polymer's resistance to crack formation. Lauke *et al.*<sup>5</sup> proposed that if the second-phase particles are sufficiently small, they will remain dispersed within the matrix without separating. They further suggested that the size of the second-phase particles in toughened epoxy resins governs the trade-off between strength reduction and toughness enhancement. As a result, numerous approaches can be employed to control and design the resin structure, aiming to strike a balance between reinforcement and toughening. These strategies include modifying existing toughening agents,<sup>6</sup> incorporating nanofillers for toughening, utilizing liquid crystal polymers,<sup>7,8</sup> designing block copolymers, synthesizing hyperbranched polymers, constructing topological network structures, and exploiting dynamic reversible chemical bond interactions to dissipate energy.

This work provides a comprehensive review of the strategies and methodologies for the simultaneous reinforcement and toughening of thermosets, including epoxy resins,<sup>9–11</sup> polybenzimidazole resins,<sup>12–14</sup> polyurethane resins,<sup>15,16</sup> cyanate ester resins,<sup>17,18</sup> bismaleimide resins,<sup>19–21</sup> unsaturated polyester resins,<sup>22–24</sup> and others. The objective is to consolidate approaches that enable thermosets to achieve improved toughness while retaining strength, and to summarize the underlying toughening mechanisms. Ultimately, this review aims to offer insights and strategies for enhancing the toughness and strength of other thermosets, based on the findings related to the aforementioned resin types.



**Zhaobin Tang**

*performance engineering plastics, the study of copolymerization, modification, and applications of polyamides, as well as the polymerization, modification, and application technologies of bio-based materials.*

*Zhaobin Tang received his PhD in Chemistry from the School of Chemistry and Chemical Engineering, Lanzhou University, in 2009. In the same year, he joined the Ningbo Institute of Materials Technology and Engineering, Chinese Academy of Sciences, as a postdoctoral researcher. He is currently conducting research at the Ningbo Institute of Materials Technology and Engineering, with research interests including the modification of high-*



**Yanlin Liu**

*Yanlin Liu obtained her PhD in Materials Science and Engineering from the School of Materials Science and Engineering, Beijing Institute of Technology, in 2018. Since 2019, she has been engaged in research at the Ningbo Institute of Materials Technology and Engineering, Chinese Academy of Sciences, where she holds a position as a researcher. Her primary research focuses on the synthesis of monomers, polymerization, functional modification, and recycling of green and sustainable polymer materials.*



## 2 Synchronous reinforcement and toughening: methods, mechanisms and challenges

### 2.1 Epoxy resin

Epoxy resin is one of the most promising thermosets, offering numerous advantages such as strong adhesion, a dense molecular structure, low curing shrinkage, and high tensile and compressive strengths. These properties have led to its widespread use in applications such as anticorrosive coatings, adhesives, semiconductors, encapsulation materials, electrical insulation, and high-performance composites. However, the highly crosslinked structure of epoxy resin limits its plastic deformation, and the volume shrinkage during the curing process generates internal stresses, which compromise its resistance to crack initiation and propagation. The methods for simultaneously toughening and strengthening epoxy resin can be broadly categorized into two types: heterogeneous toughening and homogeneous toughening.

Heterogeneous toughening arises from changes in free energy during the curing process, leading to phase separation between the modifier and the epoxy resin at the submicron or micron scale. This approach includes the use of thermoplastics (TPs), core-shell polymers (CSPs), liquid crystal polymers (LCPs), block copolymers (BCPs), nanoparticles (NMs), and interpenetrating/semipermeating network structures (IPNs/SIPNs). Enhancing interfacial interactions is critical to achieving effective heterogeneous toughening and strengthening. In contrast, homogeneous toughening involves the use of bio-based materials or hyperbranched polymers, with the modifier uniformly dispersed throughout the resin matrix. In this case, there is no secondary phase or phase separation at the micro or nanoscale, facilitating the simultaneous strengthening and toughening of the epoxy resin.

**2.1.1 The incorporation of TPs for simultaneous reinforcement and toughening.** During the curing process of epoxy resin, TPs with good compatibility, such as polysulfone and polyetheretherketone, form dual-continuous phases, phase inversion, and particle/matrix phases with epoxy resin. The toughening and strengthening mechanisms involve the uniform and dense distribution of phase-separated particles within the epoxy resin matrix, which enhances the material's stiffness. The toughness of the blend is further improved through crack bridging and crack pinning effects, resulting in simultaneous toughening and strengthening.<sup>25</sup> Since the 1980s,<sup>26</sup> TPs with good compatibility have been employed to enhance and toughen epoxy resin by forming interpenetrating networks or nano-sized dispersed phases.<sup>27</sup> Conversely, thermoplastics with poor compatibility introduce reactive functional groups (such as  $-NH_2$ ,  $-COOH$ , and  $-OH$ ) into the epoxy crosslinking structure as side or end groups. These functional groups participate in the curing and crosslinking reactions, improving the compatibility between the thermoplastics and thermosets. This approach reduces stress concentration, while simultaneously enhancing the system's toughness and impact strength. Liu *et al.*<sup>28</sup> introduced hydroxyl-terminated

phenolphthalein polyethersulfone (PESC-OH), which can react with epoxy groups, and chlorine-terminated PESC (PESC-Cl) in another sample. Experimental results showed that, compared to PESC-Cl, PESC-OH led to a 15.2% improvement in impact strength and a 5.5% increase in flexural strength. As shown in Fig. 1(b), scanning electron microscopy (SEM) revealed that after the introduction of  $-Cl$  and  $-OH$  groups, the fracture surface became uneven, indicating that the material underwent ductile fracture, thus enhancing toughness. In Fig. 1(a), it can be observed that the ductile microphase particles hinder fracture through mechanisms such as cavitation, pinning, and bridging. The introduction of reactive functional groups facilitates interactions with the resin, improving the compatibility between the toughening agent and the resin, preventing phase separation. This enables uniform and efficient stress transfer when the material is subjected to external forces, resulting in improved reinforcement and toughening effects.'

In addition to improving the compatibility between thermoplastic polymers and epoxy resins, the introduction of rubber particles alongside thermoplastic resins can result in toughening and strengthening through a synergistic effect. Zhao *et al.*<sup>29</sup> utilized carboxyl-terminated butadiene-acrylonitrile copolymer (CTBN) and thermoplastic particulate poly(ether ketone) (PEK-C) to toughen epoxy resin. As shown in Fig. 2(a), the flexural strength and modulus of the EP/PEK-C toughened system increased by 13% and 11%, respectively. This enhancement can be attributed to the presence of numerous benzene rings and polar ketone groups in the PEK-C molecular chain, which imparts greater rigidity to the chain. Fig. 2(b) illustrates the impact strength of the four systems, where the unmodified EP exhibits the lowest impact strength, indicating the poorest toughness. In contrast, the impact strength of the EP/PEK-C/CTBN system is significantly improved, showing a 342% increase

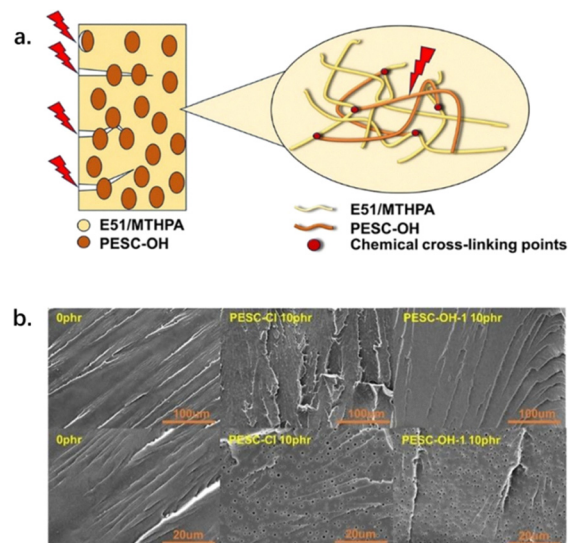


Fig. 1 (a) Schematic model of toughening mechanisms of the epoxy/PES blends, (b) SEM of the impact fracture surface of the material after curing (enlarged by a factor of 1000 or 4000). Reproduced from ref. 28 with permission from American Chemical Society, Copyright [2024].





Fig. 2 (a) The effects of PEK-C and CTBN on the flexural strength and flexural modulus of EP. (b) The impact strength value of each toughening system. Reproduced from ref. 29 with permission from Elsevier, Copyright [2024].

compared to pure EP. The liquid rubber reacted with EP to form flexible block copolymers, while PEK-C formed a co-continuous phase structure with EP. When both components acted synergistically, the “island” structure of the rubber particles bridged cracks, pinned them, and dissipated energy through shear yielding. The rigid molecular chains of PEK-C enhanced interfacial bonding and induced plastic deformation, thereby achieving a synergistic toughening effect that simultaneously improved both the strength and toughness of the epoxy resin.

**2.1.2 Block copolymers (BCPs) for reinforcement and toughening.** The block copolymers consist of compatible blocks that interact with the epoxy resin matrix and incompatible blocks, which form a nanophase-separated structure. Under external stress, the flexible blocks improve the overall ductility, thereby enhancing the toughness of the material. The nanophase-separated structure contributes to the reinforcement of the material's rigidity through mechanisms such as crack tip blunting, cavitation, debonding, limited shear yielding, and crack bridging. This synergistic effect leads to a simultaneous improvement in both the strength and toughness of the epoxy resin. In the 1990s, Könczöl *et al.*<sup>30</sup> were the first to employ block copolymers for toughening epoxy resin. They demonstrated that only a small amount of block copolymer was required to achieve significant toughening and strengthening effects, while maintaining the  $T_g$  and Young's modulus. Zhang *et al.*<sup>31</sup> introduced hydroxyl-containing reactive blocks (BPADA-HAB) and non-reactive blocks (BPADA-ODA) into the system. During the curing process of polyimide with epoxy resin, chemical bonds were formed. The addition of 5% BPADA-ODA/HAB resulted in a 184% increase in impact strength, a 150% increase in tensile strength, and a 65% improvement in fracture toughness (KIC). The reactive blocks reduced the crosslinking density, thereby enhancing the ductility and toughness of the matrix. The nanophase-separated structure, with a uniform dispersion of approximately 50 nm, further improved the material's rigidity through mechanisms such as crack deflection, interfacial stress transfer, and energy dissipation *via* thermoplastic phase deformation.

By manipulating the composition and structure, it is possible to control self-assembly or reaction-induced phase separation, leading to the formation of various nanostructures (*e.g.*,

spherical, rod-like, lamellar, vesicular, and worm-like micelles), each contributing to distinct toughening and strengthening effects. Chen *et al.*<sup>32</sup> designed a “brush-coil-tripartite block copolymer” (BCP), comprising a brush-like core of polydimethylsiloxane (PMAPDMS), coil-like polystyrene (PS) segments, and crosslinkable poly(glycidyl methacrylate) (PGMA) chains. At a mere 1 wt% concentration, the material exhibited a 1.5-fold increase in strength and a twofold enhancement in toughness. The spherical aggregates resulting from phase separation of the BCP act as physical barriers, impeding crack propagation through crack capture and deflection, thereby improving the material's toughness (Fig. 3). The PGMA segments form covalent crosslinks with the epoxy resin, strengthening the interfacial bonding between the BCP and the matrix, and ensuring effective stress transfer. During tensile testing, microcracks form around the spherical aggregates, dissipating energy *via* crack propagation and branching, while the elastic deformation of the rubbery core further absorbs energy. Through the synergistic effects of physical barriers, chemical crosslinking, and energy dissipation, this BCP effectively toughens and strengthens the epoxy resin.

**2.1.3 The addition of nanomaterials for simultaneous reinforcement and toughening.** Nanofillers, such as nano-core-shell polymers, graphene, nanoclay, carbon nanotubes, nano- $\text{Al}_2\text{O}_3$ , and nano- $\text{SiO}_2$ , experience stress concentration under external forces, leading to the formation of silver streaks and shear yielding, which effectively absorb significant amounts of energy. During crack propagation, these nanofillers inhibit fracture by facilitating mechanisms such as crack bridging and energy dissipation. Furthermore, the high specific surface area of the nanoparticles improves interfacial adhesion with the matrix, thereby enhancing effective stress transfer. This results in considerable energy absorption, simultaneously contributing to both the strengthening and toughening of the material.<sup>33</sup> Even a small amount of nanofillers can achieve substantial strengthening and toughening effects, with key factors including uniform dispersion, surface treatment, or functionalization. Moreover, the shape, size, volume fraction, aspect ratio, surface modification,  $T_g$ , and crosslinking density of the nanofillers are critical in determining the overall performance of the epoxy resin (Fig. 4).





Fig. 3 (a) ECC/IBOA 60 : 40 wt/wt mixed resin and its blends with the BCP (1 wt%), (b) DLP printed dog bone samples of the ECC/IBOA mixed resin, (c) modulus, (d) failure strength and (e) toughness of the cured samples ( $p$  value is 0.033). Reproduced from ref. 32 with permission from Elsevier, Copyright [2023].



Fig. 4 (a) SEM image of a microhardness indent showing the crack lengths and zigzag failure patterns, (b) the GNP crack-bridging toughening phenomenon, (c) low magnification SEM image of the A4Z fractured surface showing the grain boundary cracks (marked by blue arrows) and (d) the high-magnification SEM image showing well bonded matrix grains in the A4Z0.5G hybrid nanocomposite. Reproduced from ref. 34 with permission from Elsevier, Copyright [2020].

There are two primary strategies to enhance the interaction between nanofillers and the resin matrix, thereby promoting the dispersion of nanofillers. The first approach involves weak physical interactions, such as van der Waals forces and hydrogen bonding, which reduce voids between the nanofillers and the matrix, ultimately improving the mechanical properties. The second approach relies on the formation of strong chemical covalent bonds between the nanofillers and the matrix, further strengthening the interaction.<sup>35</sup> Zhang *et al.*<sup>36</sup> grafted rigid chitosan (CS) and flexible poly(ethylene glycol diglycidyl ether) (EGDE) onto the surface of graphene oxide (GO), forming a bilayer with uniform thickness. This modification significantly improves the dispersion of GO in epoxy resin, reducing

agglomeration. The incorporation of 0.1 wt% GO-CS-EGDE enhances the tensile strength and impact strength of epoxy resin by 36.2% and 54.3%, respectively, while also increasing the elongation at break by 102.7%. The combination of the rigid structure and flexible crosslinked network creates a gradient modulus interface, which alleviates modulus mismatch and facilitates uniform stress transfer. Additionally, the bilayer reduces van der Waals forces between the nanomaterials, leading to more homogeneous dispersion, with agglomerates reduced from 35  $\mu\text{m}$  to less than 5  $\mu\text{m}$ , thereby minimizing stress concentration (Fig. 5).

Toughening and strengthening of epoxy resin can also be achieved through the incorporation of nanocore-shell polymers (CSPs). Typically, a “soft core-hard shell” structure is utilized, where the hard shell, often composed of a plastic outer layer, demonstrates good compatibility with the resin matrix.<sup>37</sup> The uniformly dispersed CSPs induce microcrack deflection, void growth, and plastic deformation, with the rough fracture surface effectively dissipating energy. The core-shell particles can be engineered to control both the particle size and volume fraction of the second phase. This leads to the debonding of CSP particles from the matrix, followed by the growth of plastic voids and the formation of shear bands. When the shell thickness is maintained within a critical range, both strengthening and toughening effects can be achieved simultaneously.<sup>38,39</sup> Moreover, nanomaterials can exhibit synergistic effects when combined with other modifiers, effectively overcoming the limitations of these modifiers while preserving their advantages.

Rubber toughening of epoxy resin<sup>40</sup> is a straightforward and efficient approach to improve its mechanical properties. Commonly used rubber modifiers include carboxyl-terminated butadiene-nitrile copolymer (CTBN), hydroxyl-terminated butadiene-nitrile copolymer, and amine-terminated butadiene-nitrile copolymer. The small size and high number of rubber particles enable efficient energy dispersion during impact, effectively suppressing crack propagation.<sup>41,42</sup> However, the formation of



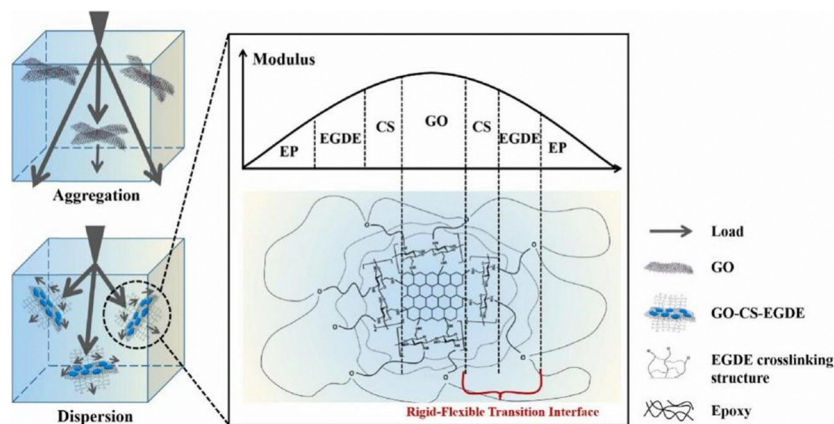


Fig. 5 Sketch map of the rigid-flexible interface and stress transfer of GO-CS-EGDE composites. Reproduced from ref. 36 with permission from Elsevier, Copyright [2022].

micron-scale second phases often results in a significant reduction in modulus and strength. The incorporation of nanoparticles can generate a synergistic effect, enhancing both the toughness and strength of the resin.<sup>43,44</sup> Liang *et al.*<sup>45</sup> optimized the synergistic toughening of epoxy resin using CTBN and nanosized cerium oxide (n-CeO<sub>2</sub>). The optimal composition was found to be 20 wt% CTBN and 1 wt% n-CeO<sub>2</sub>, resulting in increases in impact strength, flexural strength, and tensile strength by 462%, 136%, and 110%, respectively. In this system, the rubber and nanoparticles formed a dual-phase dispersion, with the rubber phase absorbing impact energy and inhibiting crack propagation. n-CeO<sub>2</sub> improved crack resistance through both its nano-effect and interfacial bonding, while the synergistic interaction between the two components optimized the phase separation structure and energy dissipation efficiency. This mechanism facilitated crack deflection and plastic deformation, thereby achieving both strengthening and toughening of the epoxy resin.

**2.1.4 LCPs for reinforcement and toughening.** LCPs as a secondary phase, enhance the toughness and strength of materials primarily through their unique rigid-flexible structure. The flexible segments, through mechanisms such as chain slip, yielding, and plastic deformation, absorb and dissipate energy, thereby improving the material's toughness. In contrast, the rigid crystalline structure reinforces the material, leading to a synergistic effect that simultaneously strengthens and toughens the resin. The incorporation of liquid crystal polymers into the epoxy resin matrix can achieve substantial enhancement and toughening with minimal addition. These polymers exhibit exceptional properties, including high strength, high modulus, and self-reinforcement. The introduction of liquid crystal polymers not only does not adversely affect the  $T_g$  and other mechanical properties, but may also enhance the thermodynamic performance.<sup>46,47</sup> Two primary approaches for toughening are employed: one involves integrating liquid crystals as a curing agent into the epoxy system, while the other entails the direct synthesis of liquid crystal epoxy resins.

During the curing process of liquid crystal epoxy resins, a highly oriented structure is formed.<sup>48</sup> When exposed to external

forces, this structure facilitates crack deflection, while the bridging effect effectively impedes crack propagation.<sup>49</sup> Fan *et al.*<sup>50</sup> successfully synthesized a bio-based liquid crystal epoxy resin (THBR-EP) by precisely tuning the length of the alkyl side chains. With the addition of only 2.5 wt% THBR-EP, the impact strength of the blend system was enhanced to 48.8 kJ m<sup>-2</sup>. The liquid crystals, with their ordered crystalline structure, crosslink with the epoxy resin matrix to form a network structure, which results in excellent compatibility and imparts superior overall properties to LC-EP. The size of the dispersed liquid crystal phase plays a crucial role in the toughening process (Fig. 6). Liu *et al.*<sup>51</sup> enhanced the toughness by constructing a multi-scale phase structure through careful control of the liquid phase elastomer (PBDPS) content, ranging from the nanometer to micrometer scale. At a content slightly below 1%, micron-level phase separation was observed, which effectively increased the tensile strength of epoxy resin by 20.7%. When the content was increased to 11.1 wt%, sub-micron phase separation occurred, leading to the highest impact strength of 35.6 kJ m<sup>-2</sup>, three times that of pure EP, while fracture toughness improved by 85.0%. The tensile strength reached 82.4 MPa. However, as the content was further increased, micron-level phase separation emerged, resulting in a slight decrease in toughening efficiency and a significant deterioration in tensile strength. At 11.1 wt%, the strong interfacial interactions between the nanometer-scale PBDPS domains and the epoxy resin matrix enhance the entanglement and slip between the two phases, thereby dissipating more fracture energy and improving the material's strength. The smaller particle spacing results in higher interaction efficiency between the sub-micron liquid crystal elastomer spheres, the matrix, and adjacent regions. This effectively induces various toughening mechanisms, such as plastic deformation and shear yielding, leading to the most significant enhancement in toughness.

**2.1.5 The incorporation of siloxane for simultaneous reinforcement and toughening.** Siloxanes are oligomeric and polymeric compounds characterized by repeating Si-O-Si backbone units.<sup>52</sup> The Si-O-Si chains exhibit outstanding thermal





Fig. 6 Curing mechanisms of blended systems. Reproduced from ref. 50 with permission from Elsevier, Copyright [2024].

stability and flexibility,<sup>53</sup> which improve the flowability of the rigid epoxy resin network and enhance its toughness. However, the poor compatibility between the flexible segments of traditional polysiloxanes and the epoxy resin matrix results in a reduction in the strength of the epoxy resin. The incorporation of epoxy groups onto the siloxane side chains, in combination with hydroxyl, amino, and epoxy end groups, improves compatibility and facilitates the formation of a dual-continuous phase<sup>54</sup> that aids in stress transfer. This mechanism plays a crucial role in the toughening effect of modified siloxanes on epoxy resins. In efforts to further enhance the toughening of epoxy resins, dynamic siloxane materials have been introduced. Ma *et al.*<sup>55</sup> employed a unique terminal hydroxyl polyborosiloxane compound (STG) as a toughening agent. When the STG content reached 15%, the elongation at break and impact strength of the epoxy resin increased by 40% and 8.1%, respectively, compared to pure epoxy resin. The inherent high flexibility of the Si–O long chains in STG, when introduced into the epoxy resin network, significantly enhanced its toughness. The dynamic B–O bond undergoes induced hardening at high strain rates, and upon stress release, the Si–O long chains recover their flexibility. This dynamic, reversible “soft–hard” transition demonstrates excellent energy dissipation capability, thereby improving the strength of the epoxy resin. The synergistic combination of these factors enables STG to simultaneously enhance both the toughness and strength of the material.

High molecular weight supramolecular polysiloxanes can be structured as block copolymers consisting of soft siloxane segments and rigid supramolecular units. The mechanical strength of these polysiloxanes increases with higher coordination bond association energy. Enhancing the graft density of supramolecular motifs and the crosslinking density of the supramolecular polymer network further strengthens the material properties of supramolecular polysiloxanes formed from graft copolymers.<sup>56</sup> Polyhedral oligomeric silsesquioxane (POSS) features a cage-like core primarily composed of Si–O–Si bonds, with eight external organic functional groups that can be designed as epoxy, amino, hydroxyl, or other groups, offering multiple reactive sites. The cage structure provides dual functions of reinforcement and energy absorption,<sup>57</sup> facilitating the simultaneous toughening and strengthening of epoxy

resins. Li *et al.*<sup>58</sup> introduced epoxy-functionalized octavinylsil-sesquioxane (EOVS) into epoxy resins. With the addition of 1% EOVS, the tensile strength and impact strength of the resin reached a maximum of 58.2 MPa and 11.3 kJ m<sup>-2</sup>, respectively, surpassing those of pure epoxy resin (47.2 MPa, 9.4 kJ m<sup>-2</sup>). The multiple epoxy groups in EOVS increase the crosslinking density, improve dispersion, and enhance the stress-bearing capacity. The flexible Si–O bonds reduce internal stress within the resin, thereby improving its toughness and resulting in increased tensile and impact strengths of the epoxy resin. As shown in Fig. 7, the use of NH<sub>2</sub>-POSS-CF for toughening and strengthening epoxy resin (EP) takes advantage of the channel structure of POSS, which provides ample free volume. This, combined with the grafted flexible siloxane chains, effectively dissipates stress and enhances the toughness of EP. The reactive groups at the end of the POSS chains react with siloxane, forming chemical bonds that improve the compatibility between the siloxane and the EP matrix, leading to a significant increase in the strength of the resin matrix. This results in the reinforcement and toughening of epoxy resin through the siloxane POSS structure.<sup>59</sup>

**2.1.6 Designing the topological network structure to achieve simultaneous reinforcement and toughening.** The construction of IPNs/SIPNs facilitates the entanglement of different polymer molecules, resulting in stable combinations of various components and the formation of microphase separation during the reaction process. The toughening and strengthening mechanism arises from the deflection and branching of cracks induced by the microphase structure, which enhances material toughness. As stress is transferred from one network to another, energy dissipation occurs, contributing to the overall toughness. A uniform network structure promotes more effective and uniform stress transfer, thereby improving the material's strength while achieving both toughening and strengthening simultaneously. The complex crosslinked network structure generates a synergistic effect, in which the polymer with favorable mechanical properties forms the cross-linked network, further enhancing its performance.

The interpenetrating structure enhances the miscibility and compatibility between the two components, combining the advantages of both polymers to achieve improved toughening and strengthening.<sup>60</sup> Pei *et al.*<sup>61</sup> introduced dynamic ester bonds into



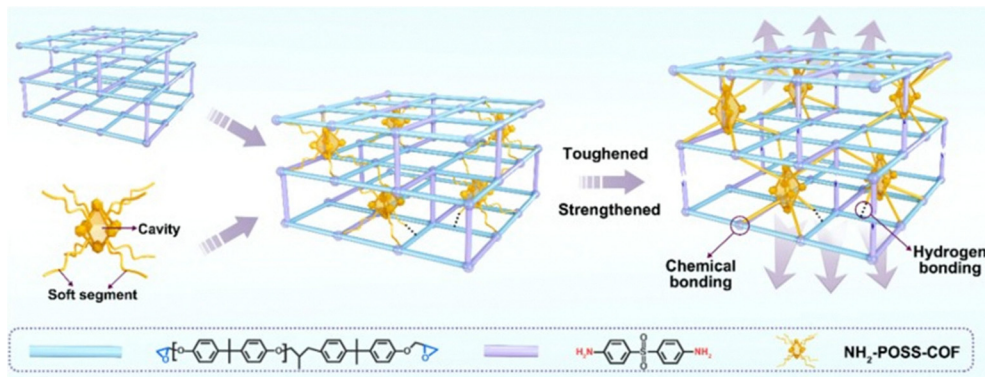


Fig. 7 Schematic diagram of  $\text{NH}_2$ -POSS-COF toughened and strengthened EP. Reproduced from ref. 59 with permission from Elsevier, Copyright [2025].

the SIPN framework. The rigid crosslinked network structure, coupled with the integration of hydrogen bonds, resulted in a tensile toughness and impact strength of  $13.8 \text{ MJ m}^{-3}$  and  $52.3 \text{ kJ m}^{-2}$ , respectively, reflecting increases of 70% and 588%. The original resin's single-network structure restricted stress transfer, making it more susceptible to stress concentration and fracture. In contrast, the introduction of an interpenetrating network structure enables more effective stress transfer and distribution, thereby improving fracture resistance. The abundant hydrogen bonds and flexible entangled chains function as sacrificial bonds and dissipative domains, shifting the energy dissipation mechanism from covalent bond rupture to hydrogen bond sacrificial action and the stretching of flexible chains (Fig. 8).

The morphology of microphase separation plays a crucial role in determining the mechanical properties of IPNs. Xie *et al.*<sup>62</sup> synthesized a diamine crosslinking agent containing boric acid esters (NBN) and incorporated dynamic borate ester

bonds into epoxy resin. When the molar content of NBN in the total amine was 25%, the material achieved a maximum elongation of 375%, a tensile toughness of  $108.4 \text{ MJ m}^{-3}$ , and a tensile strength of 41.0 MPa, demonstrating outstanding rigidity and toughness. During the reaction process, polymers with pendant butoxypropyl chains were generated, and self-assembly resulted in the formation of a layered microphase structure. This structure was locked within the network as a secondary phase separation. Each phase domain served as a crack initiation site, and the greater the number of phase domains, the stronger the mechanical properties and the more effective the stress dissipation, ultimately leading to exceptional toughness.

**2.1.7 The introduction of hyperbranched polymers (HBPs) enhances strength and toughness.** In 1996, Soerensen first introduced hyperbranched epoxy resins (HBPs), and their toughening mechanisms were classified into two types: phase

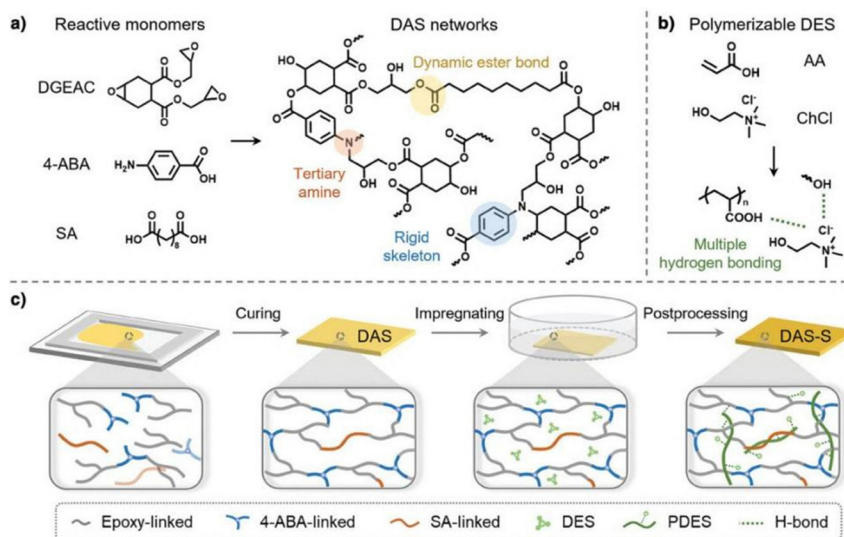


Fig. 8 Schematic illustration of the development of a DAS-S network. (a) Chemical structures of the reactive monomers DGEAC, 4-ABA, SA, and the synthetic route of the cross-linked network. (b) Composition and molecular structure of DES. Upon heating, DES undergoes thermal polymerization to form a linear poly(deep eutectic solvent) (PDES). (c) The curing process of SIPN containing dynamic ester bonds. Reproduced from ref. 61 with permission from John Wiley and Sons, Copyright [2025].



separation toughening and *in situ* toughening. The phase separation toughening mechanism results in fractured EP exhibiting a morphology with sea-island and dimple-like structures, which absorb a substantial amount of impact energy and promote the formation of yielding cavities. However, this mechanism also leads to a decrease in mechanical strength. In contrast, the *in situ* toughening mechanism involves a uniform structure devoid of phase separation, allowing for the simultaneous toughening and strengthening of thermosets. The *in situ* toughening mechanism is based on the ability of uncrosslinked hyperbranched polymers to form voids that deform under external loading, leading to the formation of fibrils.<sup>63</sup> This process absorbs more energy, preventing the rapid initiation and propagation of cracks in thermosets. A distinctive feature of this mechanism is the appearance of fibrillar structures on the fracture surface, as shown in Fig. 9. This is linked to the cavity structure of the hyperbranched polymers, which plays a crucial role in the enhancement and toughening of EP.

Modifying the chemical structure of hyperbranched polymers by incorporating rigid structures, such as hexahydro-s-triazine, carbamate, and phosphaphenanthrene groups, facilitates the simultaneous enhancement of both toughness and strength in the resin.<sup>64</sup> Li *et al.*<sup>65</sup> introduced hydroxyl-terminated hyperbranched poly(aryletherketone) (HBPAEK-OH) into epoxy resin, where the interaction between the hydroxyl groups and the epoxy resin interface improved interfacial bonding strength, thereby enhancing the tensile and flexural properties. Yu *et al.*<sup>66</sup> synthesized a highly branched silicone epoxy resin (QSiE) and incorporated 6 wt% of QSiE into the epoxy resin. This modification led to a 1.31-fold increase in impact strength, while the elongation at break of QSiE-6 reached 4.37%, representing a 93.4% improvement compared to DGEBA. This modification not only enhanced the material's toughness but also maintained its rigidity. The introduction of rigid side groups strengthens the rigidity and cohesive energy density between networks enriched with aromatic rings.



Fig. 9 Fracture surface morphology of (a) EP<sub>0</sub>, (b) EP<sub>2.5</sub>, (c) EP<sub>5</sub> and (d) EP<sub>7.5</sub>. Reproduced from ref. 63 with permission from Elsevier, Copyright [2023].

The hyperbranched structure forms additional chain entanglements with the epoxy matrix, creating anchor points within the matrix that restrict network movement, thereby increasing the resin's strength. The incorporation of hyperbranched polymers into the resin also generates numerous intramolecular cavities that facilitate shear yielding and molecular motion during fracture, contributing to enhanced material toughness (Fig. 10). Furthermore, some studies have integrated topological structures into hyperbranched polymers,<sup>67–69</sup> designing microscopic structures that organize the resin network more systematically. This results in more uniform stress transfer and distribution, thereby achieving the dual objectives of enhancing both strength and toughness.<sup>70</sup>

Research on the mechanical properties of epoxy resins has primarily focused on incorporating rigid chemical groups and designing hyperbranched microstructures. However, the influence of internal void defects and free volume characteristics has often been overlooked. An increase in free volume can result in crack blunting and energy dissipation, which in turn contributes to crack insensitivity and shear yielding. Liu *et al.*<sup>72</sup> were the first to accurately measure and demonstrate the controllability of the free volume characteristics in epoxy resins. As shown in Fig. 11, the dispersion of Bn with an ellipsoidal topology into the entangled chains of DGEBA fills the excess free volume, thereby enabling the controllability of free volume. The study found that a reduction in the relative free volume fraction, the size of free volume cavities, and the distribution of the average cavity diameter initially enhances the mechanical properties, but eventually leads to a decline. Conversely, an increase in the average diameter of the cavities induces stress concentration, resulting in a continuous deterioration of mechanical performance. By precisely controlling the shape, size, and number of cavities, as well as the free volume characteristics, both the strength and toughness of the resin can be simultaneously enhanced. In the case of hyperbranched polymers, the synergistic effects of their topology, free volume properties, good compatibility, rigid chemical structure, and high crosslinking density contribute to the toughening and strengthening of EP.

**2.1.8 The introduction of “sacrificial bonds” to enhance strength and toughness.** “Sacrificial bonds” refer to dynamic, reversible chemical bonds characterized by weak interactions that enable them to break before covalent bonds, thereby dissipating a significant amount of energy. In 2017, Filippidi *et al.*<sup>73</sup> inspired by mussels, introduced sacrificial metal coordination bonds into the epoxy resin network. Their study demonstrated that the stiffness of the resin increased without compromising its ductility. The toughening mechanism relies on non-covalent bonds and the associated nanoscale domains, which enhance stiffness by restricting the mobility of the network. These non-covalent bonds are capable of breaking prior to the rupture of covalent or stronger bonds, such as those in folding domains. The dynamic reversibility of these “sacrificial bonds” allows them to reconnect after breaking, thereby dissipating energy through transitions between different configurations. This process results in the simultaneous enhancement of both the strength and toughness of the resin.



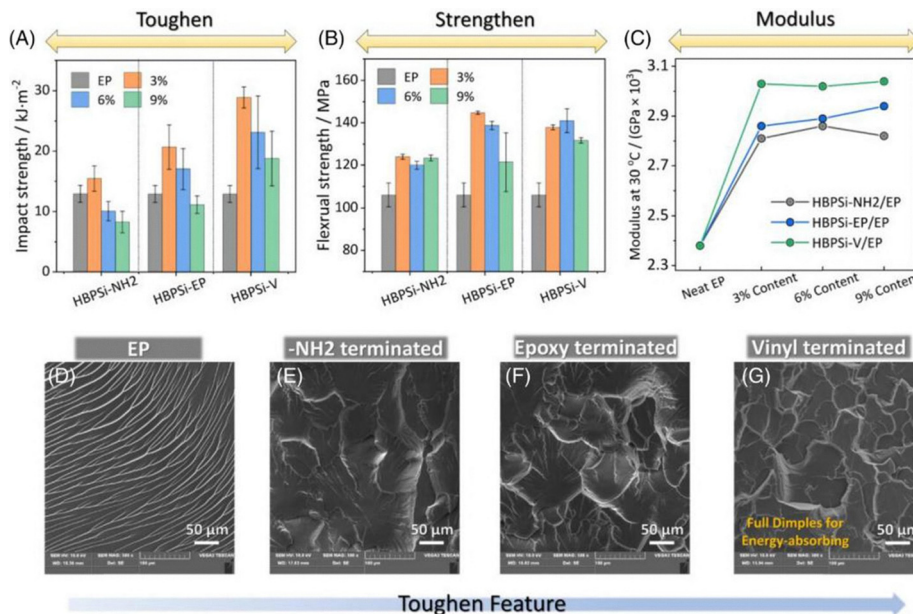


Fig. 10 The mechanical performance test of (A) impact strength, (B) flexural strength, and (C) modulus at 25 °C; (D)–(G) SEM photographs indicate the impact tough fracture from native EP to HBPSi-NH2/EP, HBPSi-EP/EP, HBPSi-V/EP. Reproduced from ref. 71 with permission from John Wiley and Sons, Copyright [2023].

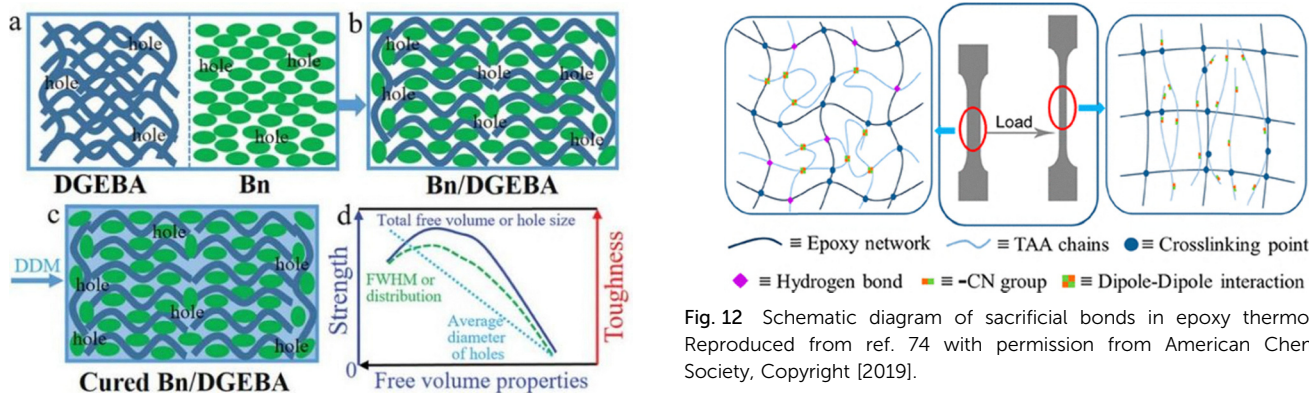


Fig. 11 Process of performance improvement on Bn/DGEBA copolymers. (a) Bn can homogeneously disperse into the DGEBA matrix due to its good compatibility, resulting from the same epoxy groups, (b) the ellipsoidal topological shape of Bn provides excellent flowability and rheological properties, enabling Bn to easily penetrate and fill the gaps between DGEBA chains, thereby densifying the free volume and hole size, (c) after curing, molecular threading and interlocking further minimize the free volume and hole diameter, leading to the formation of a high-performance copolymer. Reproduced from ref. 72 with permission from John Wiley and Sons, Copyright [2023].

The introduction of polar groups into flexible linkages facilitates the formation of hydrogen bonds, which, upon breaking, release the stored length of the flexible chains. This mechanism results in increased elongation before fracture. In 2019, Xiao *et al.*<sup>74</sup> introduced cyano groups into tung oil-based toughening agents (TAA). EP-TAA-30 incorporates cyano groups, while EP-TA2-30 incorporates carboxyl groups. EP-TAA-30 exhibited a significant improvement in fracture elongation and

toughness, with an impact strength reaching 76.7 kJ m<sup>-2</sup>. These results demonstrate that the introduction of cyano groups enables the formation of sacrificial bonds in tung oil-based materials through dipole–dipole interactions and hydrogen bonding. The presence of these bonds enhances the mechanical properties of the resin, achieving simultaneous reinforcement and toughening. The mechanism, as illustrated in Fig. 12, shows that under external stress, the sacrificial bonds break, absorbing substantial energy while releasing the flexible tung oil-based chains, thereby achieving the synchronous reinforcement and toughening of the epoxy resin.

These findings clearly demonstrate that leveraging non-covalent bonds to enhance and strengthen the epoxy resin network is a viable strategy.<sup>75</sup> Additionally, the introduction of non-covalent interactions, such as hydrogen bonding, metal coordination, and host–guest interactions, offers an effective approach to addressing the challenge of balancing toughness and strength in polymers.



## 2.2 Polybenzoxazines

Polybenzimidazole (PBz) offers several advantages, including flexible molecular design, excellent thermal stability, the absence of small molecule by-products during the curing process, and good dimensional stability.<sup>76,77</sup> These properties make PBz highly promising for applications in aerospace, electronics, automotive, and renewable energy sectors.<sup>78</sup> However, PBz exhibits a low crosslinking density and a rigid aromatic structure, which results in challenges such as high curing temperatures, brittleness, difficulty in reprocessing, and susceptibility to degradation.<sup>79</sup> In recent years, researchers have focused on modifying polybenzimidazole by altering the hydrogen bond complexes within PBz and by synthesizing hyperbranched polymers. These strategies allow for the simultaneous enhancement of both toughness and strength in PBz, addressing some of its inherent limitations

**2.2.1 The use of thermosets for synchronous reinforcement and toughening.** The incorporation of other thermosets into PBz relies on the differences in reaction types, reactivity, and chemical structures between the two resin components in the blend. During the curing process, one component preferentially undergoes polymerization, leading to phase separation and the formation of a distinct phase structure that facilitates the simultaneous toughening and strengthening of the PBz resin.<sup>80</sup> Typically, PBz is blended with a second phase *via* physical mixing,<sup>81,82</sup> which can result in phase separation that may impact the overall performance.<sup>83–85</sup> However, the use of thermosets to induce phase separation does not present this issue. Common thermosets include epoxy resins,<sup>86,87</sup> polybenzimidazole,<sup>88</sup> and bismaleimide resin.<sup>80</sup> In 2007, Kumar *et al.*<sup>89</sup> synthesized a PBz monomer containing two allyl groups, which reacted with bismaleimide. By promoting the formation of an interpenetrating IPN structure, they effectively addressed the compatibility issues between different polymers, resulting in a more homogeneous PBz/BMI blend. Similarly, Xu *et al.*<sup>90</sup> prepared an IPN consisting of diamine-based polybenzimidazole (PDMB) and polyhexahydrotriazine (PHT) through sequential polymerization. The PDMB/PHT-0.8 blend exhibited a fracture elongation of 12.40% and a tensile strength of 118.67 MPa, representing increases of 284% and 190%, respectively, compared to pure PHT. Molecular hydrogen bonds between the networks enhanced compatibility, and scanning electron microscopy revealed that the IPN structure exhibited a uniform micro-phase separation morphology. This IPN achieved simultaneous improvements in both mechanical and thermal properties through the synergistic effects of intermolecular hydrogen bonding and the interpenetrating network structure. The thermosetting resin forms a miscible system with an interpenetrating network structure, and its phase structure and composition ratio, curing reaction sequence, curing temperature, and monomer structure all influence its formation. This system can exhibit various phase structures, including homogeneous, sea-island, and co-continuous phase structures. The homogeneous structure typically results in brittle fracture, with minimal toughening effects, while the co-continuous phase structure demonstrates significant enhancement in both strength and toughness. The phase structure achieves

toughening and strengthening through mechanisms such as void shear yielding, particle-induced crack initiation, particle tearing energy absorption, and rivet effects, which dissipate a considerable amount of energy and hinder crack propagation, thereby enhancing the material's toughness and strength.

**2.2.2 The modification of monomer structures to improve toughness and strength.** The molecular design of phenolic and amine components, selected from various monomers derived from polybenzimidazole, involves the incorporation of polymerizable groups<sup>91</sup> such as allyl, propargyl, diethynyl, *o*-phthalonitrile, bismaleimide, and benzimidazole. Furthermore, the introduction of suitable amines can introduce flexible structures within the polybenzimidazole network, potentially inducing phase separation.<sup>92,93</sup> By precisely controlling the chemical composition and phase separation morphology of the prepolymer, the toughness of polybenzimidazole can be significantly enhanced (Fig. 13).<sup>94</sup> Zheng *et al.*<sup>95</sup> introduced three lauryl fatty acid chains (DLA-la) into the oxazine monomer, where the flexible fatty acid chains provide internal plasticization to the resin. These chains act as placeholders, reducing the crosslinking density, which improves ductility and enhances toughness. The hydrogen bonds formed by the amide linkages tend to break before the covalent bonds, while the flexible chain segments at the interfaces effectively buffer the applied load and redistribute stress, thereby enhancing the material's strength. This strategy results in the simultaneous toughening and strengthening of the resin.

A multifunctional prepolymer containing benzoxazine units was designed and synthesized using a chemically induced phase separation strategy. By modulating the ratio of soft to hard segments, the mechanical properties of the benzoxazine can be tailored to achieve both toughening and strengthening. Zhao *et al.*<sup>96</sup> enhanced the mechanical properties of benzoxazine by adjusting the ratio of flexible ODM to rigid MXDM. When the molar ratio of ODM to MXDM was 1 : 1, the elongation reached 10.55%, and the tensile strength increased to 82.67 MPa, representing improvements of 86% and 128%, respectively, compared to pure benzoxazine resin. Hou *et al.*<sup>97</sup> synthesized end-hydroxy poly(arylether nitrile) (PEN-OH) with varying molecular weights and incorporated it into the benzoxazine resin structure. When the molecular weight of PEN-OH was approximately  $3 \times 10^5$  and its content was 20%, the impact strength increased from  $40 \text{ kJ m}^{-2}$  to  $89 \text{ kJ m}^{-2}$ . By adjusting



Fig. 13 Modulation of prepolymer chemical composition and phase separation morphology modulates the mechanical properties of benzoxazines. Reproduced from ref. 94 with permission from Elsevier, Copyright [2011].





Fig. 14 (a) The stress–strain curves, (b) impact strength curves, (c) bending strength curves, (d) bending modulus curves, and (e) toughening mechanism diagram for different contents of poly(BZ-PEN<sub>n</sub>)/GFs. Reproduced from ref. 97 with permission from Elsevier, Copyright [2025].

the length of the PEN-OH segments, both the toughness and stiffness of the resin could be finely tuned. The flexible segments of the material absorb or offset part of the impact energy, while the high rotational freedom and interactions between segments reduce stress concentration and improve toughness, facilitating effective dispersion of external impact energy. Meanwhile, the rigid segments preserve the material's stiffness (Fig. 14).

**2.2.3 Modifying the hydrogen bond network to enhance toughness and strengthen the material.** PBz features a stable six-membered hydrogen-bonded Mannich-bridged phenol structure. Due to the low crosslinking density of benzoxazine, the hydrogen bonds within the polymer significantly influence the structure–property relationship. The mechanism for toughening and strengthening associated with hydrogen bond modification lies in the ability of these bonds to break and reorganize, thereby dissipating energy and enhancing the toughness of benzoxazine. Simultaneously, hydrogen bonds act as crosslinking points, increasing the crosslinking density and thereby improving the material's strength.<sup>98</sup> The toughening and strengthening effects of benzoxazine can be enhanced by adjusting the type and strength of the hydrogen bonds. Zhao *et al.*<sup>99</sup> incorporated the 2-ureido-4[1H]-pyrimidinone (UPy) dimer, which contains quadruple hydrogen bonds, into a benzoxazine (BA-a) system. The impact strength of all modified resins

was found to exceed that of pure benzoxazine. This enhancement is attributed to the stronger energy dissipation effect of multiple hydrogen bonds compared to conventional hydrogen bonds, as the fracture of multiple hydrogen bonds requires more energy. Additionally, the strength of hydrogen bonds significantly influences the mechanical properties of benzoxazine. Zhang *et al.*<sup>100</sup> introduced amide bonds into the main-chain benzoxazine, resulting in the formation of stronger hydrogen bonds compared to those in traditional benzoxazine. The tensile strength, tensile modulus, and elongation at break of PBz-dia were 107 MPa, 4.0 GPa, and 3.8%, respectively, representing improvements of 197%, 100%, and 100% compared to conventional PBz. The hydrogen bonds formed by the amide groups exhibit higher bond energy, enabling them to absorb more fracture energy, thereby providing enhanced toughening and strengthening effects.

Additionally, the dynamic hydrogen bonds can spontaneously reorganize after fracture, dissipating energy and restoring the material's strength. However, the modification of hydrogen bonds in PBz may adversely affect certain mechanical properties, such as  $T_g$  and modulus. Zhu *et al.*<sup>101</sup> introduced a physically interlocked polyrotaxane (PR) with epoxy groups (EPR), which strongly interacts with the PBz matrix, facilitating good molecular-scale dispersion. This interaction leads to a more uniform network, preventing significant stress concentration. The sliding of CD rings on the EPR molecules within the PBz network improves ductility and reduces the activation energy for molecular-scale motion, achieving simultaneous toughening and strengthening while preserving the  $T_g$  and modulus (Fig. 15).

**2.2.4 The introduction of a hyperbranched structure to achieve synchronous reinforcement and toughening.** Hyperbranched polymers (HBPs) can enhance the toughness of resins by inducing both heterogeneous and homogeneous morphologies. Modifying the microstructure of HBPs improves the mechanical properties of resins, achieving simultaneous strengthening and toughening. The toughening and strengthening effects of hyperbranched polymers on epoxy resins arise from a combination of factors, including crosslinking density, free volume, intermolecular voids, hyperbranched topological structure, and good compatibility. These factors enable uniform enhancement and toughening of the resin without inducing phase separation, representing an *in situ* toughening and strengthening mechanism.<sup>102</sup> Hyperbranched benzoxazine, with its highly branched structure, excellent reactivity, limited chain entanglement, abundant terminal groups, and internal cavities,<sup>103</sup> ensures effective energy transfer between the hyperbranched polymer and the benzoxazine matrix. Additionally, it induces compressive stress through extensive shear deformation or yielding, further enhancing the material's toughness (Fig. 16).

Hyperbranched polymers can be synthesized through various reactions, including condensation reactions (esterification, etherification), click reactions (thiol–ene, thiol–epoxy, thiol–isocyanate, *etc.*), addition reactions, and grafting reactions. These processes facilitate the precise control of the physical structure at the microscopic scale. By regulating the internal chemical structure,



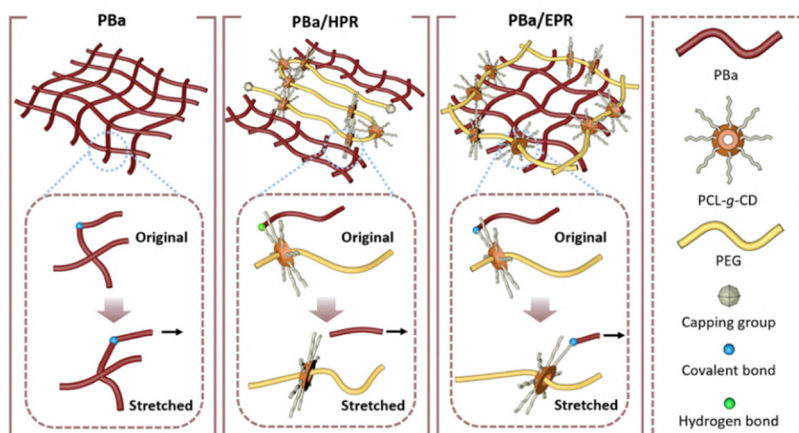


Fig. 15 Schematic of possible molecular mechanisms responsible for the observed improvement in ductility. Neat PBa shows a rigid crosslinked network. PBa/HPR with movable crosslinks of PCL-g-CD supported by intermolecular H-bonding, which is destroyed during stretching. PBa/EPR with movable cross-links of PCL-g-CD and supported by both covalent and intermolecular H-bonding to provide more extensive sliding motion of PCL-g-CD upon stretching. Reproduced from ref. 101 with permission from Elsevier, Copyright [2023].

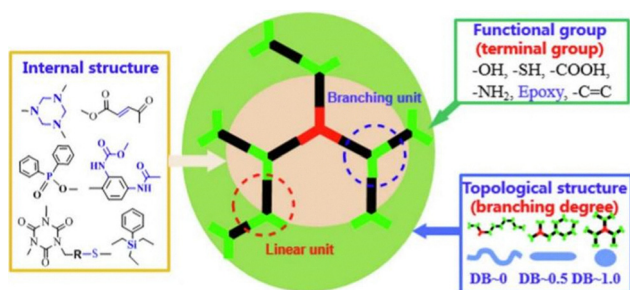


Fig. 16 Schematic diagram of the structure of hyperbranched polymers. Reproduced from ref. 104 with permission from Elsevier, Copyright [2022].

functional groups, topological arrangement, and aggregation state, the properties of hyperbranched polymers can be effectively tailored. Zhang *et al.*<sup>105</sup> introduced various types of ions into hyperbranched polymers to modify the resin properties. The cationic ion AMIM<sup>+</sup>, which exhibits higher catalytic activity, increased the crosslinking density of the cured resin, leading to enhanced mechanical performance. Specifically, the tensile, bending, and impact strengths were improved by 61.2%, 58.0%, and 67.2%, respectively. In hyperbranched polymers, the highly branched main-chain structure and three-dimensional spherical configuration facilitate energy absorption through impact deformation. Hu *et al.*<sup>106</sup> synthesized four types of triphenolamine-based hyperbranched benzoxazine copolymers using bifunctional benzoxazine (BA-a). The fracture surfaces of all four thermoset copolymers exhibited a “silk-like” structure, which significantly enhanced the strength and toughness of the benzoxazine. Among these, the incorporation of a large number of flexible ether bonds and alkyl segments into BA-a *via* polyetheramine improved the impact resistance. The flexible segments enhanced the sliding ability of the molecular chains and their energy dissipation capacity during impact. As a result, the hyperbranched polymer demonstrated superior deformation ability, leading to higher tensile and impact strengths.

### 2.3 Unsaturated polyester

Unsaturated polyesters (UP) are cost-effective,<sup>107</sup> in high market demand, exhibit fast curing rates, and offer excellent aging resistance, making them the most widely utilized thermosets in polymer processing.<sup>108,109</sup> However, the dense crosslinked network of UP resins results in poor resistance to crack initiation and propagation, leading to relatively high brittleness. To enhance toughness, it is common practice to incorporate toughening agents.<sup>110</sup>

Long-chain dicarboxylic acids or long-chain diols, such as hexadecanedioic acid, polyethylene glycol, and tung oil, are frequently employed as monomers for toughening agents. However, the use of these agents often leads to a significant reduction in the tensile strength and hardness of the resulting materials.<sup>111</sup> To achieve a more effective improvement in mechanical properties, the incorporation of rigid segments is necessary. Another approach involves blending unsaturated polyester with thermoplastic elastomers. The elastomers improve the toughness of the rigid network without compromising the hardness or other mechanical properties of the base polymer. However, this method necessitates improving the compatibility between the elastomer and the resin matrix.<sup>112</sup> For instance, the inclusion of butadiene-acrylonitrile copolymers with terminal functional groups (such as carboxyl, amine, acrylic, thiol, and hydroxyl groups) can enhance the interfacial adhesion between the toughening agent and the UP resin during the curing process.

**2.3.1 The incorporation of both rigid and flexible segments to improve strength and toughness.** The toughening mechanism of unsaturated polyester resin (UPR) relies on the presence of flexible groups, which facilitate the movement and free rotation of the matrix chains. This promotes uniform crack initiation, effectively disperses impact energy, and enhances the toughness and ductility of the resin.<sup>113</sup> Simultaneously, the incorporation of rigid segments increases the resin's strength. Tu *et al.*<sup>114</sup> introduced a small amount of



rigid, bio-based 2,3-butanediol (2,3-BDO) units into the molecular chain of polybutylene furan-2,5-dicarboxylate (PBF). At a 2,3-BDO content of 4 mol%, the resulting copolyester exhibited a tensile strength of 67.0 MPa and an elongation at break of 556.2%. The addition of rigid segments improved the material's mechanical properties, particularly its strength. Furthermore, the toughness and strength of the material can be further optimized by controlling the ratio of soft to hard segments, the degree of unsaturation in the polyester, and the regularity of the network structure. Georgina<sup>115</sup> *et al.* achieved ionic association within the hard segments by precisely controlling the sodium coordination in the monomer sequence, thereby creating physically crosslinked rigid domains that enhance both mechanical strength and toughness. When the sodium neutralization degree reached 75%, the tensile strength increased to 20 MPa (a 35-fold improvement compared to the unmodified sample), while the toughness reached 260 MJ m<sup>-3</sup> (Fig. 17).

The double bonds undergo crosslinking reactions with UPR, thereby increasing the crosslinking density of the system. This enhanced crosslinking, in combination with the stress dissipation facilitated by the flexible chains, contributes to both the toughening and strengthening of the material.<sup>23</sup> Zhang *et al.*<sup>116</sup> improved the toughness of UPR by adjusting the unsaturation level of phosphonate ester oligomers. In a system containing 22 wt% phosphonate ester, the impact strength and elongation at break were increased by 460% and 200%, respectively. The C=C bonds in polyethylene (PE) participated in the curing of UPR, and the introduction of flexible phosphonate ester ether segments (P-O-C) promoted the plastic deformation of the matrix, enhancing its energy dissipation capability and achieving simultaneous toughening and strengthening. In addition to increasing the crosslinking density of the UPR network, the regularity of the network also plays a crucial role in influencing the toughening effect. Rouhi *et al.*<sup>117</sup> demonstrated that adding 2 wt% core-shell particles and 1 wt%  $\gamma$ -alumina ( $\gamma$ -Al<sub>2</sub>O<sub>3</sub>) to the composite material significantly improved its toughness, tensile strength, elastic modulus, and flexural strength by 41%, 16%, 50%, and 20%, respectively, compared to the UPR/CSR

system containing only core-shell particles. This improvement was attributed to the  $\gamma$ -alumina, which enhanced the network regularity by controlling the free radical curing reaction, further reinforcing the toughening effect.

**2.3.2 The introduction of a second phase to enhance strength and toughness.** The incorporation of rigid particles, such as graphene oxide, carbon nanotubes, and graphene, into thermosets improves both the elastic modulus and thermal stability.<sup>118</sup> The simultaneous presence of rigid and soft particles generates a synergistic effect that enhances the strength and toughness of polymer composites. The toughening mechanism is primarily attributed to the inherent toughness of the second-phase components or the phase-separated structures formed during the curing process of the thermosetting resin. Soft particles undergo deformation to absorb impact energy, thereby increasing fracture toughness,<sup>119</sup> although they may reduce the resin's elastic modulus, strength, and glass transition temperature ( $T_g$ ).<sup>120</sup> In contrast, rigid particles enhance material strength through mechanisms such as crack tip blunting, cavitation, debonding, limited shear yielding, and crack bridging. The combined effect of these two phases leads to the simultaneous enhancement of both strength and toughness. Gao *et al.*<sup>121</sup> synthesized ion-liquid-modified MXene (I-MXene) using a chemical grafting method and incorporated it with ammonium polyphosphate (APP) as a synergistic flame retardant into UPR. The tensile strength of the I-MXene/APP/UPR composite was 18.44% higher, and the elongation at break improved by 16.3% compared to the APP/UPR composite. Ion-liquid modification enhanced the dispersion of I-MXene. Furthermore, the incorporation of rigid nanoparticles such as nano-SiO<sub>2</sub>, nano-Al<sub>2</sub>O<sub>3</sub>, TiO<sub>2</sub>, and nano-clay<sup>122</sup> can also improve toughness without compromising the material's mechanical or thermal properties.

## 2.4 Bismaleimide

Bismaleimide (BMI), a high-performance engineering plastic, demonstrates exceptional mechanical properties, high transition temperature, and superior heat resistance and thermal

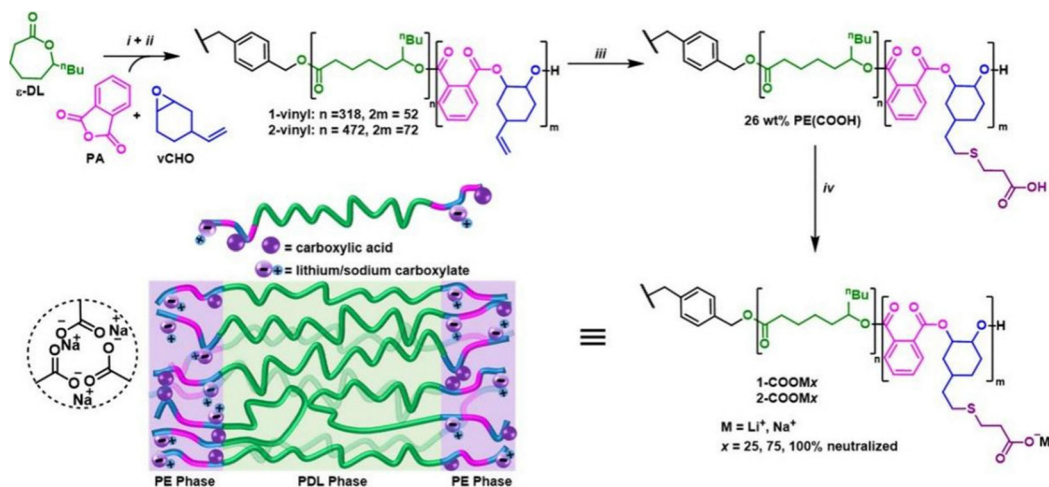


Fig. 17 Synthesis of polyester ionomers. Reproduced from ref. 115 with permission from American Chemical Society, Copyright [2022].



stability, which surpass those of thermoplastic materials.<sup>123,124</sup> As a result, it has found widespread application in advanced industries such as aerospace, aircraft carriers, automobiles, and structural components. However, the highly cross-linked structure of BMI, coupled with the presence of aromatic rings in its main chain, imparts significant brittleness. Additionally, the polar carbonyl groups in BMI resins hinder the orderly arrangement of polymer chains and limit energy dissipation, making BMI more brittle and less tough compared to other thermosets. To address these limitations, various strategies have been proposed to process and toughen BMI, including the incorporation of flexible linkages, the addition of rigid particles, the modification of network structures, and copolymerization with other thermosets.

**2.4.1 Introducing flexible segments to enhance strength and toughness.** When subjected to external forces, the flexible segments are capable of undergoing torsion and deformation. The toughening and strengthening mechanism is primarily attributed to the immiscibility of the flexible segments with the BMI matrix, which induces phase separation. The rigid resin matrix undergoes plastic deformation, while a large number of fine shear bands form at the interface between the flexible phase and the matrix, facilitating energy dissipation. Furthermore, the flexible segments dissipate and transfer stress energy, preventing the shear bands from evolving into fracture lines, thereby contributing to reinforcement and toughening.

Incorporating additional flexible bonds into the network structure, typically through the inclusion of ether groups, increases the molecular degrees of freedom, which enhances the material's energy absorption capacity and, consequently, improves its impact resistance. Jiang *et al.*<sup>125</sup> achieved a synergistic enhancement of both strength and toughness in BMI resins by introducing flexible aliphatic long chains and rigid phosphorinated phenyl groups. The aliphatic long chains reduce the crosslinking density and increase the mobility of the molecular chains, while the phosphorinated phenyl groups improve interface stress dispersion through polar interactions. As a result, the tensile strength of the material remains around 33 MPa (Fig. 18).

**2.4.2 The addition of rigid particles to enhance strength and toughness.** Rigid particles exhibit high modulus and strength. The disparity in modulus between the rigid particles and the resin matrix leads to deformation incompatibility under external forces, causing interfacial debonding and the formation of numerous microvoids. This process is the primary mechanism through which rigid particles enhance the toughening and strengthening of the resin.<sup>126–128</sup> Zheng *et al.*<sup>129</sup> functionalized graphene nanosheets (rGO/WS<sub>2</sub>) with polyamide-type polyphosphazene to reinforce bismaleimide (BMI) resins. At 0.8 wt% and 0.6 wt% loading of PHbP@rGO/WS<sub>2</sub>, the impact strength and flexural strength of the BMI composites reached peak values of 21.2 kJ m<sup>-2</sup> and 185.7 MPa, respectively, representing improvements of 82.8% and 52.0% compared to pure BMI. The  $\pi$ - $\pi$  interactions between rGO and WS<sub>2</sub> promote chemical bonding, while the amino groups at the edges of the nanosheets react with the matrix to form covalent bonds, thereby

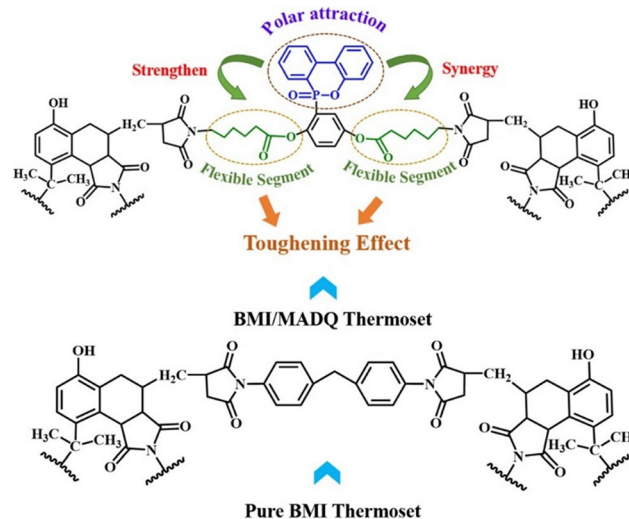


Fig. 18 Schematic diagram of the toughening structures in BMI/MADQ thermosets. Reproduced from ref. 125 with permission from Elsevier, Copyright [2022].

enhancing interfacial bonding strength. This enables the matrix to effectively transfer the applied stress to the nanosheets. Additionally, the presence of WS<sub>2</sub> prevents the aggregation of rGO sheets, improving the dispersion of the nanomaterials and enhancing the mechanical properties of the resin, resulting in reinforcement and toughening.

Zhou *et al.*<sup>130</sup> designed and synthesized a novel maleimide-functionalized tris(triazine) polyphosphazene microsphere (PPM). PPM was modified *via* acylation with 6-maleimido-hexanoic acid chloride, improving its interfacial compatibility with BMI. The impact strength of the composites increased by 97.5%, and the modulus of PPM was significantly higher than that of the BMI matrix. As rigid particles, PPM induces interfacial plastic deformation and disperses microcracks, thereby dissipating impact energy and reinforcing and toughening the resin. In summary, it can be observed that rigid particles enhance toughness and strength primarily by dissipating a significant amount of energy through the formation of microvoids. However, these particles are prone to aggregation, which can lead to stress concentration and adversely affect the material's performance. By employing methods such as intercalation and blending, chemical bonds can be formed between the organic and inorganic phases, reducing particle aggregation and improving compatibility, thereby achieving enhanced toughening and strengthening effects.

**2.4.3 Modifying the network structure to enhance strength and toughness.** BMI possess a high degree of crosslinking and a rigid main molecular chain, which contributes to their increased brittleness and poor impact resistance. However, by modifying the network structure, these mechanical properties can be effectively regulated.<sup>131</sup> The mechanism behind the enhancement and toughening lies in the increased crosslinking density within the network, which enhances the resin's rigidity. The introduction of flexible segments enables rotational energy dissipation, while an increase in free volume facilitates energy



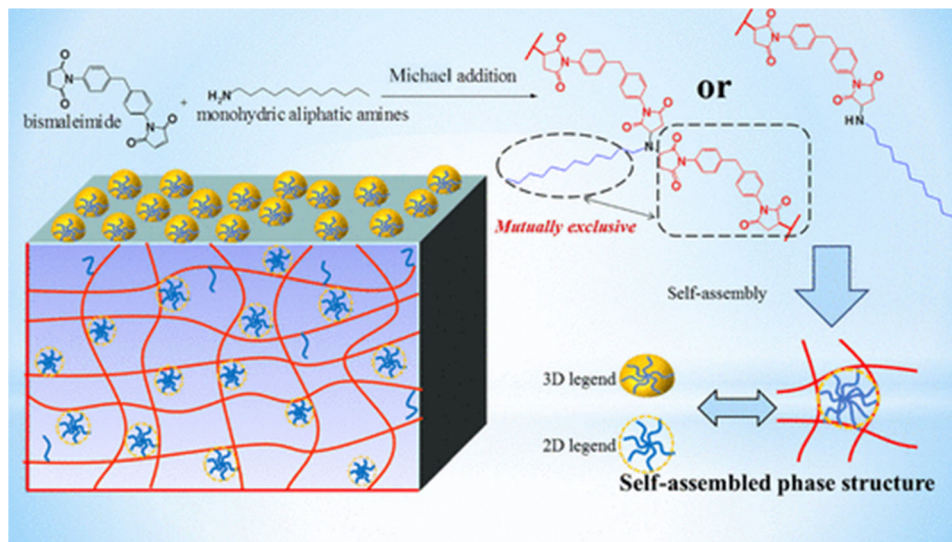


Fig. 19 Schematic diagram of the self-assembled phase structure of a modified BMI resin with flexible aliphatic chains. Reproduced from ref. 140 with permission from American Chemical Society, Copyright [2019].

absorption by the molecules, thereby improving the impact resistance of the resin matrix (Fig. 19).<sup>132</sup> Additionally, the formation of a topological network, where different polymer molecules interweave, allows the components to complement each other in terms of performance, effectively achieving both reinforcement and toughening of the BMI.<sup>133</sup> Han *et al.*<sup>134</sup> developed an amino-functionalized organic framework (sN-MIL) for the toughening modification of bismaleimide resin (BD). At a sN-MIL loading of 0.3 wt%, the impact strength and fracture toughness (KIC) of the BD composites increased by 1.70 and 1.58 times, respectively, compared to pure BD resin. The amino groups<sup>135</sup> of sN-MIL co-polymerize with the imide groups of the bismaleimide resin, thereby increasing the cross-linking density. Meanwhile, the porous structure of sN-MIL introduces free volume, which facilitates segmental motion, disperses stress, and reduces the density of polar groups. The nanometer-sized sN-MIL particles are uniformly dispersed, inducing crack bridging and deflection, which suppresses crack propagation. Zhou *et al.*<sup>136</sup> designed and synthesized two star-shaped allyl-functionalized phosphazene small molecules. At low concentrations of HECF, the allyl group predominantly contributes to toughening by participating in the formation of the bismaleimide crosslinked network. This reduces the cross-linking density and, in turn, enhances toughness, although at the expense of rigidity. When the HECF content reaches 5 wt%, the combined effects of allyl group toughening and the reinforcing effect of the phenyl rings result in both improved strength and toughness.<sup>137–139</sup>

## 2.5 Cyanate ester resin

Cyanate ester resins (CEs) exhibit exceptional high temperature resistance, mechanical, adhesive, and dielectric properties, making them suitable for high-performance applications such as high-speed printed circuit boards, satellite antenna systems, and radar domes. Cyanate ester resins typically contain

phenolic derivatives with two or more cyanate ester functional groups, which form a highly crosslinked network structure under the influence of a catalyst or through self-catalysis. The presence of a significant number of triazine rings, aromatic rings, or rigid ester rings imparts impact resistance superior to that of bismaleimide and epoxy resins. However, the highly crosslinked network structure necessitates toughening and reinforcement modifications. Common methods for enhancing toughness include the incorporation of thermoplastic polymers and the construction of interpenetrating network structures.

**2.5.1 The introduction of thermoplastic polymers to enhance strength and toughness.** During the curing process, thermoplastic polymers precipitate from the cyanate ester resin matrix, forming a microphase structure that enhances the interfacial compatibility between the CEs and the modifier.<sup>141</sup> By adjusting the molecular weight of the thermoplastic toughening agents, a double-continuous or inverted structure is formed, leading to significant improvements in toughness and impact resistance through mechanisms such as plastic deformation and crack deflection. This results in enhanced strength and toughness of the resin.<sup>142,143</sup> Jayalakshmi *et al.*<sup>144</sup> utilized polyetherimide (PEI) to toughen CE. When the PEI content was 18–20 wt%, the composite material formed an interpenetrating network with a co-continuous structure. The tensile strength reached 372–376 MPa, representing a 27–28% increase compared to pure CE, while the compressive strength improved by 40%, demonstrating excellent mechanical properties. The inverted structure, with PEI as the continuous phase, enhanced both toughness and strength through mechanisms of plastic deformation and crack deflection.

Amirova *et al.*<sup>145</sup> prepared a high-temperature-resistant phenolic CE/PES (polyethersulfone) blend system and investigated the effects of PES molecular weight and content on the phase separation behavior of the system. When low molecular weight PES (2603 MP, with hydroxyl groups) was blended with CE,



a spherical dispersed phase structure was formed. In contrast, high molecular weight PES (4100 MP, 5003 MP) resulted in a co-continuous or inverted structure. At 20 phr PES content, the low molecular weight PES system with hydroxyl groups exhibited a fracture toughness (KIC) of 0.72 MPa m<sup>1/2</sup>, a 132% increase compared to pure CE, while the fracture energy (GIC) increased to 117 J m<sup>-2</sup>. This demonstrated the synergistic toughening enhancement mechanisms of crack pinning and plastic deformation.<sup>146</sup> The introduction of cyano groups improves interfacial compatibility, where the chemical reaction between the cyano groups and the cyanate ester groups enhances interfacial interactions. This leads to a reduction in particle size and suppresses excessive phase separation, preventing the formation of a continuous phase. The combined effects of improved interfacial bonding and particle refinement collectively enhance the energy absorption capability.<sup>147</sup>

**2.5.2 The introduction of an interpenetrating network structure to enhance strength and toughness.** The formation of an interpenetrating polymer network structure leads to molecular chain entanglement, creating a system of forced compatibility that results in a more uniform distribution of stress and enhanced energy transfer efficiency. Concurrently, this network induces the separation of new microphases during the curing process, facilitating crack deflection and branching. Wang *et al.*<sup>148</sup> modified bisphenol A dicyanate ester (BADCy) resin with epoxy-terminated fluorinated poly(ether ketone) (EFPAEK). At an EFPAEK content of 20 wt%, the bending strength and impact strength increased by 32.5% and 159.3%, reaching 131.8 MPa and 30.6 kJ m<sup>-2</sup>, respectively. The epoxy groups in EFPAEK reacted with the cyanate ester groups to form an interpenetrating network, thereby enhancing compatibility. The flexible ether bonds within EFPAEK facilitated molecular chain mobility, while the rigid arrangement of phenyl rings within the molecular chains contributed to the resin's rigidity, thus achieving both enhancement and toughening of the cyanate ester. Zhou *et al.*<sup>149</sup> synthesized a novel epoxy-fluorinated linear random copolymer, P(PFS-co-GMA), *via* reversible addition-fragmentation chain transfer (RAFT) polymerization. This copolymer formed a semi-interpenetrating network structure with the cured cyanate resin. The bending strength and impact strength improved to 122.4 MPa and 14.6 kJ m<sup>-2</sup>, respectively, reflecting increases of 23.1% and 49.0% compared to pure BADCy resin (99.4 MPa and 9.8 kJ m<sup>-2</sup>). The semi-interpenetrating network structure enhanced the mechanical properties of the resin. The fluorine atoms, with their larger free volume, increased the flexibility of the chain segments within the cyanate resin system, simultaneously reinforcing and toughening the material.

## 2.6 Thermosetting polyurethane

In 2020, global polyurethane (PU) production reached approximately 24 million tons.<sup>150</sup> Polyurethane resins (PURs) are recognized for their excellent toughness and fatigue resistance, which significantly contribute to extending the service life of composite materials.<sup>151</sup> Thermosetting polyurethanes, due to their chemical resistance, customizable structure,<sup>152</sup> and

versatile mechanical properties, find widespread application in industries such as coatings, adhesives, sealants, and elastomers.<sup>153–155</sup> PU is a block copolymer consisting of both soft and hard segments. The soft segments are typically composed of oligomeric polyols, including polyester polyols, polyether polyols, and polyolefin polyols, while the hard segments primarily consist of isocyanates and small molecular chain extenders. By adjusting the types and relative proportions of the soft and hard segments, it is theoretically possible to engineer polyurethane materials with tailored properties to meet specific requirements.

**2.6.1 The addition of reinforcing fillers to enhance strength and toughness.** Commonly used rigid fillers, such as nanosilica, nanoclay, and carbon nanotubes, exhibit high modulus and strength. When subjected to external forces, the deformation mismatch between the particles and the matrix leads to particle–matrix debonding, which generates numerous micropores. This phenomenon dissipates significant amounts of energy, thereby contributing to the enhancement and toughening of the material. However, these fillers often exhibit poor compatibility with the matrix, and their dispersion is frequently insufficient, which diminishes their reinforcing effect.<sup>156,157</sup> Zhang *et al.*<sup>158</sup> employed succinylated cellulose nanofibers and chitosan nanofibers as reinforcing fillers. The acetyl amino groups in these fillers are capable of forming additional hydrogen bonds with the waterborne polyurethane (WPU) matrix, thereby facilitating the preparation of waterborne polyurethane materials with exceptional mechanical strength and toughness.

**2.6.2 The introduction of an elastic covalent network to enhance strength and toughness.** The use of an elastomeric covalent bond network to improve mechanical properties relies on the toughening and strengthening mechanism of the elastic covalent network.<sup>159</sup> This network induces phase separation, forming micro-phase particles. The dynamic covalent bonds provide a higher crosslinking density, which enhances the rigidity of the network. When subjected to external forces, the dynamic fracture of the network dissipates significant amounts of energy, resulting in improved ductility and thus enhancing toughness.<sup>160</sup> Yang *et al.*<sup>161</sup> achieved dual dynamic crosslinking through multiple hydrogen bonds and disulfide bonds to prepare amorphous transparent polyurethane/nanocellulose elastomers with excellent self-reinforced toughening performance. As shown in Fig. 20, the PTMG segments in the polyurethane exhibit good flexibility, contributing to the superior toughness of the material. The high crystallinity of 2-ureido-4[TH]-pyrimidinone (UTCNF) and the close alignment of polyurethane bonds after the stretching process facilitate the constraint and orientation of polymer chains, thereby enhancing the material. Additionally, as illustrated in Fig. 20(e), the elastomer exhibits a synergistic effect of multiple hydrogen bonds and dynamic disulfide bonds, providing a strong crosslinking interaction and energy dissipation mechanism for the three-dimensional crosslinked network. This enables energy dissipation under external forces, preventing material failure. Consequently, both the fracture strength, elongation at break, and toughness are simultaneously improved, avoiding the brittleness issues





Fig. 20 (a) Illustration of polyurethane synthesis process, synthesis of (b) UPy-TCNF, (c) prepolymer, (d) PU-SS-UTCNF, (e) Diagram of polyurethane chemical constitution. Reproduced from ref. 161 with permission from John Wiley and Sons, Copyright [2023].

commonly associated with traditional crosslinked networks or rigid fillers. The toughening and strengthening mechanism induced by hydrogen bonds primarily enhances the material's strength by increasing the physical crosslinking points. When subjected to external force, the rupture of hydrogen bonds consumes a significant amount of energy, preventing crack propagation and thus achieving toughening enhancement. Wang *et al.*<sup>162</sup> designed a supramolecular poly(urethane-urea) network (SPUUN) by utilizing the interactions between rigid and flexible supramolecular segments, which form mismatched supramolecular interactions (MMSIs). The supramolecular segments aggregate into larger clusters, and when the material is subjected to external forces, these clusters preferentially dissociate and dissipate energy. This significantly enhances the material's performance, achieving an exceptionally high tensile strength (110.8 MPa) and tensile toughness (1245.2 MJ m<sup>-3</sup>). The dynamic covalent adaptive network of dynamic bonds leverages the characteristics of dynamic covalent chemistry to simultaneously enhance and toughen the unsaturated polyester. Upon the application of external forces, the dynamic bonds

break to absorb energy and, under certain conditions, can reassemble, making this a promising approach for imparting unprecedented plasticity and reprocessability to crosslinked polymers.

**2.6.3 The introduction of rigid molecular segments to enhance strength and toughness.** The incorporation of rigid units can enhance the strength of polyurethane, while the long segments improve the material's ductility, imparting toughness and thus achieving a toughening and strengthening effect.<sup>163</sup> By controlling the crystallization behavior of the hard segment structure, the mechanical properties of the polyurethane resin can be modified and enhanced. Aguiar *et al.*<sup>164</sup> enhanced PU using halloysite nanotubes (HNTs), where the addition of 0.8 wt% acid-treated HNTs resulted in a 35% increase in interlayer shear strength and a 21% improvement in fracture toughness of the nanocomposite. HNTs influence the crystallization of the hard segments in polyurethane, forming smaller, harder, and more uniformly distributed spherulites. The regions between the spherulites exhibit greater ductility, and the fracture surface becomes rougher, leading to enhanced



energy dissipation capability. Jia *et al.*<sup>165</sup> introduced F–H bonds into two covalently crosslinked poly(urethane–urea) (CPUU) elastomers to construct dynamic nanoscale crosslinked domains. The inclusion of F–H bonds in the CPUU-FA elastomer resulted in tensile strength, elongation at break, and toughness reaching  $42.3 \pm 1.9$  MPa,  $624 \pm 28.4\%$ , and  $81.5 \pm 3.9$  MJ m<sup>-3</sup>, respectively, which represented a 1.3 and 1.5-fold improvement in mechanical strength and toughness compared to the F–H bond-free CPUU-BA. The strong electronegativity of fluorine enhances the hydrogen bonding energy, resulting in higher binding energy. This leads to greater energy dissipation when the material is subjected to external forces. Additionally, the strong interactions of the hydrogen bonds reduce the inter-chain distance, promoting  $\pi$ – $\pi$  stacking and refining the crystallized phase. This results in smaller spherulite sizes, weaker aggregation in the hard domains, and a more uniform distribution of soft and hard segments. Consequently, the more uniform distribution of hard domains and finer, harder crystalline regions in the resin significantly enhances its performance. The enhancement effect can be further controlled by adjusting the materials that induce crystallization and the energy of the hydrogen bonds (Fig. 21).

**2.6.4 Biobased structural modification for strength and toughness enhancement.** The toughness of biobased polyurethane is related to the functionality of the polyol monomers used.<sup>166</sup> Polyols with high functionality and high hydroxyl value lead to the formation of biobased polyurethanes with high crosslinking density, resulting in materials with high modulus and  $T_g$ .<sup>167</sup> When the crosslinking density is the same, stronger hydrogen bond crosslinking interactions between hard segments, along with a higher degree of crystallinity induced in the soft segments under strain, contribute to enhanced mechanical properties of the elastomer,<sup>168</sup> thereby achieving improved toughness and strength.

Castor oil (CO) naturally contains hydroxyl groups, and its hydrophobic long fatty acid chains impart flexibility and water resistance to polyurethanes or polyureas derived from CO.

However, the flexible main chain reduces the material's strength and modulus. To address this, rigid structural enhancers or increased crosslinking density are typically introduced into the polyurethane to improve its mechanical properties.<sup>169</sup> Zhou *et al.*<sup>170</sup> introduced two types of dynamic crosslinking bonds, disulfide and imine bonds, resulting in a tensile strength of  $42 \pm 2$  MPa and a fracture elongation of  $125 \pm 16\%$ . The rigid structure of aromatic amines imparts excellent strength to the polyurethane network. The recombination of the two dynamic bonds, in conjunction with the flexible long chains present in CO, leads to an increase in toughness. Lignin (DEL), with its rigid aromatic structure and numerous reactive sites,<sup>171</sup> can be used to synthesize ultra-high-performance, and tough polyurethane elastomers.<sup>172</sup> Wang *et al.*<sup>173</sup> investigated the preparation of a tough lignin-containing polyurethane elastomer (LPUes) with a reversible double-crosslinked network, utilizing the abundant polar functional groups and phenolic hydroxyls in the lignin molecule. The LPUes exhibited a tensile strength of 31.4 MPa and a fracture strain of 1528%. The double-crosslinked network formed between the DEL and the polyurethane matrix (chemical crosslinking and hydrogen bond physical crosslinking), along with the strain-induced crystallization self-reinforcement effect,<sup>174</sup> enabled the simultaneous enhancement and toughening of the polyurethane.<sup>175,176</sup> Biobased materials overcome the limitations of traditional, non-renewable materials while imparting excellent mechanical properties, making them a promising direction for future reinforcement and toughening, aligning with the trend of green development.

### 3. Conclusion and prospects

Significant advancements have been made in the toughening and reinforcement of thermosets, effectively overcoming the traditional notion that strength and toughness are mutually exclusive. Conventional toughening agents, including rubber

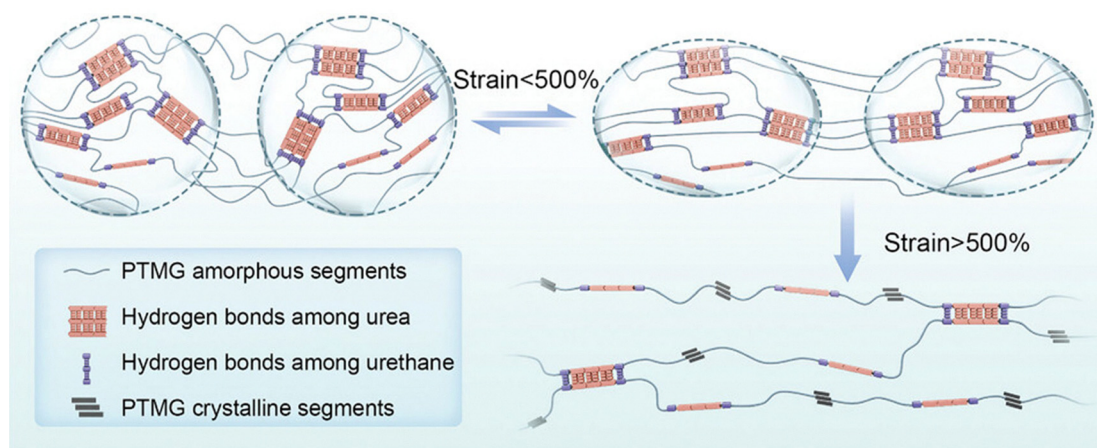


Fig. 21 Proposed mechanism of enhanced puncture resistance, tear resistance, tensile strength, and toughness of CPUU-FA. Reproduced from ref. 165 with permission from John Wiley and Sons, Copyright [2025].



elastomers, thermoplastic polymers, core-shell polymers, liquid crystal polymers, block copolymers, and nanoparticles, function as secondary-phase toughening agents. By strategically designing their molecular structures and utilizing the synergistic effects of blending two or more toughening agents, these materials achieve enhanced toughness and reinforcement. When external forces are applied, the differing moduli of the phases generate numerous shear bands around rigid particles, thereby dissipating substantial amounts of energy. This process facilitates the simultaneous enhancement of both toughness and strength in thermosets. Additionally, the incorporation of interpenetrating or semi-interpenetrating network structures allows for the tailoring of the material's microstructure, where the rigid phase contributes to strength, while the flexible network undergoes rotational energy dissipation to improve toughness. The uniformity of the network structure ensures more consistent stress transfer, resulting in superior toughening effects. In recent years, hyperbranched polymers and bio-based materials have also been increasingly applied to enhance the toughness and reinforcement of thermosets. The incorporation of hyperbranched polymers introduces numerous voids within the resin matrix, facilitating easier molecular chain mobility and thereby improving toughness. Notably, homogeneous hyperbranched systems can enhance toughness without compromising other mechanical properties, offering a balanced improvement in material performance. Based on the unique structure of certain bio-based materials, such as lignin, the introduction of sacrificial bonds dissipates a large amount of energy before covalent bond breakage, thereby enhancing the toughness and strength of thermosets. With the advancement of fields such as aerospace and renewable energy, the demands for higher mechanical strength and greener, more sustainable development of thermosets have increased. Consequently, thermosets are expected to evolve toward the following objectives:

(1) Development of thermosets with multifunctional properties such as flame retardancy, high temperature resistance, high strength, and enhanced toughness: the development of such resins addresses key challenges in high-end manufacturing sectors, aiming to overcome the limitations of single-performance materials. The focus is on achieving a synergistic balance between strength and toughness to meet the stringent material requirements in industries such as aerospace, renewable energy, and rail transportation. By precisely controlling the molecular structure, a "rigid skeleton-flexible link" micro-phase separation structure can be designed, or elements that combine both flame retardant and strengthening properties (such as phosphorus, silicon, and boron) can be introduced to enhance the overall performance.

(2) Design of thermosets with dynamic bonding structures for closed-loop recycling and material reuse: the incorporation of dynamic bonding structures imparts reprocessability and disassemblability to thermosets, properties traditionally lacking in such materials. Under specific external stimuli, the crosslinking bonds can undergo reversible breakage and reconstruction, facilitating easier recycling and processing. The introduction

of dynamic covalent bonds, such as disulfide bonds and ester exchange bonds, or the use of supramolecular chemistry to incorporate non-covalent bonds like hydrogen bonds and metal coordination bonds, enables the creation of dynamic systems that enhance material recyclability without compromising the overall resin performance.

(3) Synthesis of thermosets with enhanced toughness at low temperatures: traditional thermosets are prone to brittleness and reduced strength at low temperatures, which limits their application in high-performance fields where reliability is critical. The development of thermosets that exhibit improved toughness and strength retention at low temperatures significantly enhances the reliability and durability of components, making them more suitable for demanding environments.

(4) Exploration of bio-based resources for the development of high-performance resins as alternatives to petroleum-based resins: the utilization of bio-based resources, derived from renewable biomasses such as agricultural residues, wood fibers, and waste oils, offers a sustainable approach to reducing the cost of thermosets while decreasing dependence on petroleum resources. Converting biomass into high-performance resins not only contributes to environmental sustainability but also presents challenges in ensuring the consistent quality and performance of bio-based materials, as well as optimizing production processes to control costs.

## Conflicts of interest

There are no conflicts of interest to declare.

## Data availability

No primary research results, software or code have been included and no new data were generated or analysed as part of this review.

## Acknowledgements

Authors thank the financial support from the National Natural Science Foundation of China (52473105), the Ningbo Key Technology Development of Science and Innovation Yongjiang 2035 (2024Z102), and the National key research and development program (2022YFC2104505).

## References

- Z. Fang, H. Mu, Z. Sun, K. Zhang, A. Zhang, J. Chen, N. Zheng, Q. Zhao, X. Yang, F. Liu, J. Wu and T. Xie, *Nature*, 2024, **631**, 783–788.
- M. H. Karami, M. Kalaei, R. Khajavi, O. Moradi and D. Zaarei, *Adv. Compos. Hybrid Mater.*, 2022, **5**, 390–401.
- F. Van Lijsebetten, T. Maiheu, J. M. Winne and F. E. Du Prez, *Adv. Mater.*, 2023, **35**, 2300802.
- A. Mirmohseni and S. Zavareh, *J. Polym. Res.*, 2009, **17**, 191–201.



- 5 B. Lauke, *Compos. Sci. Technol.*, 2008, **68**, 3365–3372.
- 6 X. Fei, W. Wei, F. Zhao, Y. Zhu, J. Luo, M. Chen and X. Liu, *ACS Sustainable Chem. Eng.*, 2016, **5**, 596–603.
- 7 J. K. Choi, B. W. Lee, Y. S. Choi, B. W. Jo and S. K. Choi, *J. Appl. Polym. Sci.*, 2014, **132**, 41408.
- 8 S. Wang, S. Ma, N. Li, S. Jie, Y. Luo and X. Gao, *Eur. Polym. J.*, 2023, **196**, 112302.
- 9 S. Jahanshahi, A. Pizzi, A. Abdulkhani, K. Doosthoseini, A. Shakeri, M. C. Lagel and L. Delmotte, *Ind. Crops Prod.*, 2016, **83**, 177–185.
- 10 M. Lu, Y. Liu, X. Du, S. Zhang, G. Chen, Q. Zhang, S. Yao, L. Liang and M. Lu, *Ind. Eng. Chem. Res.*, 2019, **58**, 6907–6918.
- 11 X. Xiong, X. Guo, R. Ren, L. Zhou and P. Chen, *Polym. Test.*, 2019, **77**, 105917.
- 12 K. Tang, A. Zhang, T. Ge, X. Liu, X. Tang and Y. Li, *Mater. Today Commun.*, 2021, **26**, 101879.
- 13 L. Zhang, Y. Zhang, L. Wang, Y. Yao, J. Wu, Y. Sun, M. Tian and J. Liu, *Polym. Test.*, 2019, **73**, 208–213.
- 14 B. Zhu, X. Jiang, S. Li and M. Zhu, *Polymers*, 2024, **16**, 1255.
- 15 B. Godinho, N. Gama, A. Barros-Timmons and A. Ferreira, *Sustainable Mater. Technol.*, 2021, **29**, e00330.
- 16 X. C. Li, Y. S. Bi and G. H. Bi, *J. Appl. Polym. Sci.*, 2024, **141**, e55177.
- 17 S. Chen, L. Yuan, Z. Wang, A. Gu and G. Liang, *Composites, Part B*, 2019, **177**, 107438.
- 18 J. Jiang, Y. Zhou, C. Liu and C. Zhang, *Chem. Eng. J.*, 2025, **504**, 158840.
- 19 S. Li, H. Yan, S. Feng and X. Li, *Polym. Bull.*, 2016, **73**, 3547–3557.
- 20 S. Lu, Q. He, X. Zeng, Z. Ma, Y. Yang and X. Chen, *Polym. Eng. Sci.*, 2024, **64**, 5859–5878.
- 21 W. Pang, R. Shi, J. Wang, Q. Ping, X. Sheng, N. Li and J. Zhang, *Materials*, 2021, **14**, 4909.
- 22 M. Ahmadi, M. R. Moghbeli and M. M. Shokrieh, *Iran. Polym. J.*, 2012, **21**, 855–868.
- 23 X. Han, Y. Jin, J. Huang, H. Tian and M. Guo, *J. Polym. Environ.*, 2022, **30**, 3209–3217.
- 24 D. Li, X. Zhao, Y. Jia, L. He, X. Wang and Y. Wang, *Polym. Degrad. Stab.*, 2019, **168**, 108961.
- 25 R. Wu, X. Zhang, X. Wei, D. Jing, W. Su and S. Zhang, *New Carbon Mater.*, 2024, **39**, 681–691.
- 26 S. Lee, E. Jeong, M. Y. Lee, M. K. Lee and Y. S. Lee, *J. Ind. Eng. Chem.*, 2016, **33**, 73–79.
- 27 D. Chen, J. Li, Y. Yuan, C. Gao, Y. Cui, S. Li, H. Wang, C. Peng, X. Liu, Z. Wu and J. Ye, *Polymer*, 2022, **240**, 124518.
- 28 J. Liu, X. Zhang, H. Wang, L. Song and G. Zhou, *ACS Appl. Polym. Mater.*, 2024, **6**, 6068–6076.
- 29 Z. Wang, Y. Lai, P. Xu, J. Ma, Y. Xu and X. Yang, *Polymers*, 2024, **16**, 2775.
- 30 L. Könczöl, W. Döll, U. Buchholz and R. Mülhaupt, *J. Appl. Polym. Sci.*, 2003, **54**, 815–826.
- 31 L. Zhang, X. Zhang, X. Wei, D. Jing, W. Su and S. Zhang, *Compos. Sci. Technol.*, 2022, **230**, 109787.
- 32 R. Chen, J. Cai, K. C. H. Chin, S. Wang, A. J. Boydston, R. Thevamaran and P. Gopalan, *Giant*, 2024, **17**, 100204.
- 33 H. Gu, H. Zhang, C. Ma, X. Xu, Y. Wang, Z. Wang, R. Wei, H. Liu, C. Liu, Q. Shao, X. Mai and Z. Guo, *Carbon*, 2019, **142**, 131–140.
- 34 I. Ahmad, M. Islam, N. Al Habis and S. Parvez, *J. Mater. Sci. Technol.*, 2020, **40**, 135–145.
- 35 W. Wang, G. Zhou, B. Yu and M. Peng, *Composites, Part B*, 2020, **197**, 108044.
- 36 W. Zhang, G. Song, J. Zhu, C. Wang, H. Zheng, B. Li, Z. Yu, X. Yang and L. Ma, *Compos. Commun.*, 2022, **34**, 101262.
- 37 N. Thirunavukkarasu, H. Bhuvanewari Gunasekaran, S. Peng, A. Laroui, L. Wu and Z. Weng, *Mater. Des.*, 2023, **225**, 111510.
- 38 M. Zou, J. Chen, Z. Wei, W. Lei, J. You, J. Liu, Q. Zhang and D. Shi, *Appl. Surf. Sci.*, 2023, **614**, 156051.
- 39 W. Shi, J. Li, M. Song, Y. Han, C. Wang and Q. Ren, *J. Appl. Polym. Sci.*, 2024, **141**, e55579.
- 40 R. Thomas, D. Yumei, H. Yuelong, Y. Le, P. Moldenaers, Y. Weimin, T. Czigan and S. Thomas, *Polymer*, 2008, **49**, 278–294.
- 41 S. Bao, L. Zhu, H. Wang, H. Luo, F. Chen, W. Yu, Z. Zhang, X. Zhuang, Q. Wu, Y. Shangguan and Q. Zheng, *Compos. Sci. Technol.*, 2023, **242**, 110210.
- 42 S. L. Kirshenbaum, S. Gazit and J. P. Bell, *Rubber-Modified Thermoset Resins*, American Chemical Society, Washington, 1984.
- 43 M. Turkben, S. Kocaman, N. Özmeral, U. Soydal, A. Cerit and G. Ahmetli, *Ind. Crops Prod.*, 2023, **195**, 116490.
- 44 J. Zhang, H. Zhang, D. Yan, H. Zhou and Y. Yang, *Sci. China: Chem.*, 1997, **40**, 15–23.
- 45 D. Liang, X. Li, Y. Zhang, J. Qi and Z. Lu, *Polym. Compos.*, 2024, **46**, 3480–3495.
- 46 G. Ye, S. Huo, C. Wang, P. Song, Z. Fang, H. Wang and Z. Liu, *Polym. Degrad. Stab.*, 2023, **207**, 110235.
- 47 Y. Qi, Q. Fan, J. Li, Q. Cao, X. Pan, Y. Pan, X. Jian and Z. Weng, *Compos. Commun.*, 2023, **44**, 101771.
- 48 X. Sun, S. Chen, B. Qu, R. Wang, Y. Zheng, X. Liu, W. Li, J. Gao, Q. Chen and D. Zhuo, *Nat. Commun.*, 2023, **14**, 6586.
- 49 X. Zhao, W. Chen, X. Han, Y. Zhao and S. Du, *Compos. Sci. Technol.*, 2020, **191**, 108094.
- 50 Q. Fan, J. Li, Q. Cao, C. Gu, Q. Liu, X. Jian and Z. Weng, *Compos. Commun.*, 2024, **51**, 102068.
- 51 X. Liu, X. Luo, B. Liu, H. Zhong, D. Guo, R. Yang, L. Chen and Y. Wang, *ACS Appl. Polym. Mater.*, 2019, **1**, 2291–2301.
- 52 K. Matsumoto, Y. Oba, Y. Nakajima, S. Shimada and K. Sato, *Angew. Chem., Int. Ed.*, 2018, **57**, 4637–4641.
- 53 J. J. Chruściel and E. Leśniak, *Prog. Polym. Sci.*, 2015, **41**, 67–121.
- 54 Y. Ling, B. Qiu, X. Lei, L. Shen, H. Jin, X. Zhang, M. Liang, Y. Chen and H. Zou, *Composites, Part B*, 2024, **284**, 111675.
- 55 J. Ma, H. Wen, K. Wang, Z. Xiong, F. Yan, Z. Zhang and K. Yu, *Polym. Eng. Sci.*, 2024, **64**, 4904–4919.
- 56 B. Yi, S. Wang, C. Hou, X. Huang, J. Cui and X. Yao, *Chem. Eng. J.*, 2021, **405**, 127023.
- 57 H. Liu, M. Chai, Y. Wu, P. Zhang, M. Liu, L. Liu and Y. Huang, *Chem. Eng. J.*, 2024, **492**, 152415.



- 58 S. Li, Y. Liu, Y. Liu and Q. Wang, *Composites, Part B*, 2021, **223**, 109115.
- 59 R. Jin, Y. Zhang, D. Guo, Z. Zhou, L. Qu and B. Xu, *Composites, Part A*, 2025, **193**, 108846.
- 60 B. Wang, N. Li, Q. Bao, D. Liu, H. Guo, G. Li, G. Zheng, G. Zhang, Y. Qiao, Z. Weng and X. Jian, *Polymer*, 2023, **266**, 125619.
- 61 D. Pei, P. Wang, J. Hao, Y. Zi, O. Zhang, J. Yang, J. Tang and J. Hu, *Angew. Chem., Int. Ed.*, 2025, **64**, e202505526.
- 62 W. Wu, H. Feng, L. Xie, A. Zhang, F. Liu, Z. Liu, N. Zheng and T. Xie, *Nat. Sustain.*, 2024, **7**, 804–811.
- 63 H. Qiao, M. Chen, B. Chen, H. Zhang and B. Zheng, *Chem. Eng. J.*, 2023, **467**, 143542.
- 64 X. Liu, Y. Xiao, X. Luo, B. Liu, D. Guo, L. Chen and Y. Wang, *Chem. Eng. J.*, 2022, **427**, 132031.
- 65 S. e Li, H. Liu, H. Zhu, X. Li, H. Li, L. Shi, Y. Li, J. Yu, F. Bao, C. Zhu and J. Xu, *Eur. Polym. J.*, 2024, **210**, 112951.
- 66 M. Yu, Z. Chen, J. Li, J. Tan and X. Zhu, *Molecules*, 2023, **28**, 2826.
- 67 N. Tian, R. Ning and J. Kong, *Polymer*, 2016, **99**, 376–385.
- 68 J. Gao, B. A. Patterson, Y. Kashcooli, D. O'Brien and G. R. Palmese, *Composites, Part B*, 2022, **238**, 109857.
- 69 L. Zhong, Y. Hao, J. Zhang, F. Wei, T. Li, M. Miao and D. Zhang, *Macromolecules*, 2022, **55**, 595–607.
- 70 J. Wu, N. Liang, X. Liu, J. Cheng, Z. Xu, T. Li, M. Miao and D. Zhang, *Prog. Org. Coat.*, 2022, **165**, 106735.
- 71 Y. Zhang, J. Yuan, J. Hu, Z. Tian, W. Feng and H. Yan, *Aggregate*, 2023, **5**, e404.
- 72 X. Liu, H. Wu, W. Xu, Y. Jiang, J. Zhang, B. Ye, H. Zhang, S. Chen, M. Miao and D. Zhang, *Adv. Mater.*, 2023, **36**, 2308434.
- 73 E. Filippidi, T. R. Cristiani, C. D. Eisenbach, J. H. Waite, J. N. Israelachvili, B. K. Ahn and M. T. Valentine, *Science*, 2017, **358**, 502–505.
- 74 L. Xiao, J. Huang, Y. Wang, J. Chen, Z. Liu and X. Nie, *ACS Sustainable Chem. Eng.*, 2019, **7**, 17344–17353.
- 75 Y. Shen, B. Wang, D. Li, X. Xu, Y. Liu, Y. Huang and Z. Hu, *Polym. Chem.*, 2022, **13**, 1130–1139.
- 76 V. Duhan, N. Amarnath, S. Yadav and B. Lochab, *ACS Appl. Polym. Mater.*, 2023, **5**, 2971–2982.
- 77 N. N. Ghosh, B. Kiskan and Y. Yagci, *Prog. Polym. Sci.*, 2007, **32**, 1344–1391.
- 78 X. Zhou, F. Fu, M. Shen, Q. Li, H. Liu and Z. Song, *Adv. Sustainable Syst.*, 2023, **8**, 2300372.
- 79 S. Rimdusit, S. Pirstpindvong, W. Tanthapanichakoon and S. Damrongsakkul, *Polym. Eng. Sci.*, 2005, **45**, 288–296.
- 80 C. Shi, Q. Song, H. Wang, S. Ma, C. Wang, X. Zhang, J. Dou, T. Song, P. Chen, H. Zhou, Y. Chen, C. Zhu, Y. Bai and Q. Chen, *Adv. Funct. Mater.*, 2022, **32**, 2201193.
- 81 I. Hamerton, L. T. McNamara, B. J. Howlin, P. A. Smith, P. Cross and S. Ward, *J. Appl. Polym. Sci.*, 2014, **131**, 40875.
- 82 I. Hamerton, L. T. McNamara, B. J. Howlin, P. A. Smith, P. Cross and S. Ward, *Macromolecules*, 2014, **47**, 1946–1958.
- 83 E. Douse, S. Kopsidas, D. Jesson and I. Hamerton, *React. Funct. Polym.*, 2016, **103**, 117–130.
- 84 J. Zhou, R. Wang, X. He, C. Zhao, H. Gou and L. Zhao, *J. Polym. Eng.*, 2018, **38**, 933–943.
- 85 T. Liu, M. Xu, Z. Bai, D. Ren, X. Xu and X. Liu, *Polymer*, 2022, **260**, 125355.
- 86 H. Peng, Y. Wang, Y. Zhan, F. Lei, P. Wang, K. Li, Y. Li and X. Yang, *Eur. Polym. J.*, 2025, **222**, 113604.
- 87 M. L. Costa, S. F. M. d Almeida and M. C. Rezende, *Compos. Sci. Technol.*, 2001, **61**, 2101–2108.
- 88 Y. Wang, K. Kou, L. Zhuo, H. Chen, Y. Zhang and G. Wu, *J. Polym. Res.*, 2015, **22**, 51.
- 89 K. S. Santhosh Kumar, C. P. Reghunadhan Nair, R. Sadhana and K. N. Ninan, *Eur. Polym. J.*, 2007, **43**, 5084–5096.
- 90 Y. Xu, Z. Li, K. Zhu, X. Sun, Y. Liu, S. Xiong, Y. Wu and Y. Yang, *Polym. Degrad. Stab.*, 2022, **204**, 110103.
- 91 Y. L. Liu, C. W. Hsu and C. I. Chou, *J. Polym. Sci., Part A: Polym. Chem.*, 2007, **45**, 1007–1015.
- 92 H. Ardhyananta, M. H. Wahid, M. Sasaki, T. Agag, T. Kawauchi, H. Ismail and T. Takeichi, *Polymer*, 2008, **49**, 4585–4591.
- 93 H. Ishida and H. Y. Low, *J. Appl. Polym. Sci.*, 1998, **69**, 2559–2567.
- 94 C. Sawaryn, K. Landfester and A. Taden, *Polymer*, 2011, **52**, 3277–3287.
- 95 Y. Zheng, Z. Qian, H. Sun, J. Jiang, F. Fu, H. Li and X. Liu, *J. Polym. Sci.*, 2022, **60**, 2808–2816.
- 96 Y. Zhao, Y. Xu, Q. Xu, F. Fu, Y. Zhang, T. Endo and X. Liu, *Macromol. Chem. Phys.*, 2018, **219**, 1700517.
- 97 J. Hou, J. Ye, X. Liu, S. Liu, L. Tong and X. Liu, *Mater. Today Commun.*, 2025, **45**, 112207.
- 98 H. Liang, H. Liu, Y. Chen, Y. Cui, T. Bu and Z. Wang, *J. Mater. Res. Technol.*, 2024, **31**, 659–667.
- 99 S. Zhao, S. Li, H. Liu, J. Jiang, M. Wang, H. Liu, W. Wang and Z. Wang, *Adv. Compos. Hybrid Mater.*, 2022, **5**, 3057–3067.
- 100 Y. Zhang, X. Zhang, G. Zhan, Q. Zhuang and X. Liu, *Polym. Bull.*, 2024, **82**, 1973–1984.
- 101 Z. Zhu, H. Chen, X. Zhu, Z. Sang, S. A. Sukhishvili, S. Uenuma, K. Ito, M. Kotaki and H. J. Sue, *Compos. Sci. Technol.*, 2023, **235**, 109976.
- 102 X. Ma, W. Guo, Z. Xu, S. Chen, J. Cheng, J. Zhang, M. Miao and D. Zhang, *Composites, Part B*, 2020, **192**, 108005.
- 103 T. Liu, Z. Yuan, X. Wang, Q. Chen, A. A. K. Gorar, W. B. Liu and J. Wang, *React. Funct. Polym.*, 2025, **209**, 106175.
- 104 X. Mi, N. Liang, H. Xu, J. Wu, Y. Jiang, B. Nie and D. Zhang, *Prog. Mater. Sci.*, 2022, **130**, 100977.
- 105 J. Zhang, S. Chen, Q. He, P. Guo, Z. Xu and D. Zhang, *React. Funct. Polym.*, 2018, **133**, 37–44.
- 106 L. X. Hu, Z. C. Wang, Z. Y. Guo, T. Liu, Z. G. Yuan, M. Derradji, W. B. Liu and J. Wang, *J. Appl. Polym. Sci.*, 2024, **141**, e55873.
- 107 H. Abrial, R. Fajrul, M. Mahardika, D. Handayani, E. Sugiarti, A. N. Muslimin and S. D. Rosanti, *Polym. Test.*, 2020, **81**, 106193.
- 108 K. Qiu, X. Zhang, X. Liu, Z. Chen, L. Ni, Z. Chen, Y. Yu and J. Jiang, *React. Funct. Polym.*, 2025, **213**, 106266.



- 109 G. Altamura, E. Manarin, G. Griffini and S. Turri, *Eur. Polym. J.*, 2025, **228**, 113819.
- 110 A. M. Ali, M. A. Jaber and N. A. Toama, *Iraqi J. Sci.*, 2021, **62**, 1128–1134.
- 111 P. A. Jeemol, S. Mathew and C. P. R. Nair, *Polym. Eng. Sci.*, 2021, **61**, 2931–2944.
- 112 Y. Hu, W. Liu, W. Hu, F. Chu, L. Song and Y. Hu, *Chem. Eng. J.*, 2024, **501**, 157583.
- 113 D. Xu, D. Wu, T. Yu and R. Fu, *J. Appl. Polym. Sci.*, 2017, **135**, 45562.
- 114 Z. Tu, X. Zhang, J. Li, L. Li, F. Zhou, H. Ma and Z. Wei, *Eur. Polym. J.*, 2024, **220**, 113477.
- 115 G. L. Gregory and C. K. Williams, *Macromolecules*, 2022, **55**, 2290–2299.
- 116 Q. Zhang, B. Xu, H. Zhou and L. Qian, *Polymer*, 2024, **301**, 127035.
- 117 E. Rouhi, K. Bahrami and M. Poorabdollah, *Polym. Compos.*, 2025, **46**, 10908–10922.
- 118 F. Chu, Y. Hu, W. Hu, L. Song and Y. Hu, *Composites, Part B*, 2025, **294**, 112171.
- 119 Y. J. Huang, J. H. Wu, J. G. Liang, M. W. Hsu and J. K. Ma, *J. Appl. Polym. Sci.*, 2007, **107**, 939–950.
- 120 M. Ahmadi, M. R. Moghbeli and M. M. Shokrieh, *Polym. Eng. Sci.*, 2012, **52**, 1928–1937.
- 121 M. Gao, J. Wang, Y. Gao, J. Chen, L. Qian and Z. Qiao, *J. Vinyl Addit. Technol.*, 2023, **30**, 530–542.
- 122 A. Chencheni, S. Belkhir, A. F. Tarchoun, A. Abdelaziz, W. Bessa, Y. Boucheffa and D. Trache, *RSC Adv.*, 2024, **14**, 517–528.
- 123 Y. Zhou, W. Liu, W. Ye, S. Li, F. Chu, W. Hu, L. Song and Y. Hu, *Chem. Eng. J.*, 2024, **481**, 148409.
- 124 Y. Li, F. Zhang, Y. Liu and J. Leng, *Small*, 2023, **20**, 2307244.
- 125 X. Jiang, F. Chu, X. Zhou, X. Li, P. Jia, X. Luo, Y. Hu and W. Hu, *J. Colloid Interface Sci.*, 2022, **614**, 629–641.
- 126 X. Zhou, S. Qiu, J. Liu, M. Zhou, W. Cai, J. Wang, F. Chu, W. Xing, L. Song and Y. Hu, *Chem. Eng. J.*, 2020, **401**, 126094.
- 127 R. K. Jena and C. Y. Yue, *Compos. Sci. Technol.*, 2016, **124**, 27–35.
- 128 Q. Guan, L. Yuan, A. Gu and G. Liang, *ACS Appl. Mater. Interfaces*, 2018, **10**, 39293–39306.
- 129 Z. Chen, H. Yan, L. Guo, L. Li, P. Yang and B. Liu, *Composites, Part A*, 2019, **121**, 18–27.
- 130 X. Zhou, S. Qiu, F. Chu, Z. Xu and Y. Hu, *Chem. Eng. J.*, 2022, **450**, 138083.
- 131 F. Chen, H. Zhang, S. Li, Y. Chen, M. Liang, Z. Heng and H. Zou, *Compos. Sci. Technol.*, 2023, **242**, 110170.
- 132 Y. Li, F. Zhang, Y. Liu and J. Leng, *Composites, Part A*, 2023, **165**, 107328.
- 133 Z. Chen, M. Zhang, Z. Guo, H. Chen, H. Yan, F. Ren, Y. Jin, Z. Sun and P. Ren, *Composites, Part B*, 2023, **248**, 110374.
- 134 X. Han, L. Yuan, A. Gu and G. Liang, *Composites, Part B*, 2018, **132**, 28–34.
- 135 S. Niu, H. Yan, S. Li, C. Tang, Z. Chen, X. Zhi and P. Xu, *J. Mater. Chem. C*, 2016, **4**, 6881–6893.
- 136 X. Zhou, S. Qiu, L. He, X. Wang, Y. Zhu, F. Chu, B. Wang, L. Song and Y. Hu, *Chem. Eng. J.*, 2021, **425**, 130655.
- 137 Y. Niu, S. Zhao, B. Song, C. Wang, X. Cao and X. Zhang, *Mater. Des.*, 2023, **233**, 112260.
- 138 E. Richaud and J. Delozanne, *Polym. Degrad. Stab.*, 2024, **219**, 110628.
- 139 K. Ohtsuka, S. Nakao and Y. Hatanaka, *Polymer*, 2025, **320**, 127979.
- 140 Q. Zou, F. Xiao, S. Q. Gu, J. Li, D. J. Zhang, Y. F. Liu and X. B. Chen, *Ind. Eng. Chem. Res.*, 2019, **58**, 16526–16531.
- 141 A. V. Rau, S. A. Srinivasan, J. E. McGrath and A. C. Loos, *Polym. Compos.*, 2004, **19**, 166–179.
- 142 Z. Xie, Z. Li, J. Su, H. Zhao, Y. Zhang and W. Chen, *J. Phys.: Conf. Ser.*, 2025, **2956**, 012005.
- 143 Z. Li, J. Hu, L. Ma and H. Liu, *J. Appl. Polym. Sci.*, 2019, **137**, 48641.
- 144 J. Cherukattu Gopinathapanicker, A. Inamdar, A. Anand, M. Joshi and B. Kandasubramanian, *Ind. Eng. Chem. Res.*, 2020, **59**, 7502–7511.
- 145 L. Amirova, F. Schadt, M. Grob, C. Brauner, T. Ricard and T. Wille, *Polym. Bull.*, 2020, **79**, 213–225.
- 146 J. W. Hwang, S. D. Park, K. Cho, J. K. Kim, C. E. Park and T. S. Oh, *Polymer*, 1997, **38**, 1835–1843.
- 147 Y. Feng, Z. Fang and A. Gu, *Polym. Adv. Technol.*, 2004, **15**, 628–631.
- 148 C. Wang, Y. Tang, Y. Zhou, Y. Zhang, J. Kong, J. Gu and J. Zhang, *Polym. Chem.*, 2021, **12**, 3753–3761.
- 149 Y. Zhou, J. Zhang, C. Qu, L. Li, J. Kong and J. Gu, *Adv. Compos. Hybrid Mater.*, 2021, **4**, 1166–1175.
- 150 M. B. Johansen, B. S. Donslund, E. Larsen, M. B. Olsen, J. A. L. Pedersen, M. Boye, J. K. C. Smedsgård, R. Heck, S. K. Kristensen and T. Skrydstrup, *ACS Sustainable Chem. Eng.*, 2023, **11**, 10737–10745.
- 151 A. Khan, M. Naveed and M. Rabnawaz, *Green Chem.*, 2021, **23**, 4771–4779.
- 152 S. Kim, K. Li, A. Alsbaiee, J. P. Brutman and W. R. Dichtel, *Adv. Mater.*, 2023, **35**, 2305387.
- 153 Z. Lei, Z. Wang, H. Jiang, J. R. Cahn, H. Chen, S. Huang, Y. Jin, X. Wang, K. Yu and W. Zhang, *Adv. Mater.*, 2024, **36**, 2407854.
- 154 J. A. Nettles, S. Alfarhan, C. A. Pascoe, C. Westover, M. D. Madsen, J. I. Sintas, A. Subbiah, T. E. Long and K. Jin, *JACS Au*, 2024, **4**, 3058–3069.
- 155 S. A. Madbouly, *Composites, Part A*, 2023, **42**, 100835.
- 156 C. Zhang, L. Xia, B. Deng, C. Li, Y. Wang, R. Li, F. Dai, X. Liu and W. Xu, *ACS Appl. Mater. Interfaces*, 2020, **12**, 25409–25418.
- 157 J. Han, W. Zhang, M. Wei, Y. Zhu, X. Liu and X. Li, *Composites, Part B*, 2024, **284**, 111693.
- 158 S. Jang, E. M. Go, J. Kim, S. K. Kwak and J. Jin, *Composites, Part B*, 2022, **247**, 110353.
- 159 Z. Liu, Z. Fang, N. Zheng, K. Yang, Z. Sun, S. Li, W. Li, J. Wu and T. Xie, *Nat. Chem.*, 2023, **15**, 1773–1779.
- 160 F. Zeng, X. Men, M. Chen, B. Liu, Q. Han, S. Huang, H. Zhao and Y. Wang, *Chem. Eng. J.*, 2023, **454**, 140023.



- 161 W. Yang, Y. Zhu, T. Liu, D. Puglia, J. M. Kenny, P. Xu, R. Zhang and P. Ma, *Adv. Funct. Mater.*, 2023, **33**, 2213294.
- 162 L. Wang, K. Zhang, X. Zhang, Y. Tan, L. Guo, Y. Xia and X. Wang, *Adv. Mater.*, 2024, **36**, 2311758.
- 163 X. Wang, J. Xu, Y. Zhang, T. Wang, Q. Wang, Z. Yang and X. Zhang, *Polym. Chem.*, 2022, **13**, 3422–3432.
- 164 R. Aguiar, R. E. Miller and O. E. Petel, *Sci. Rep.*, 2021, **11**, 13161.
- 165 Y. Jia, C. Chu, Z. Wu, Y. Ni, S. Cao, T. Liao, C. Shi, Y. Men, J. Sun and Z. You, *Angew. Chem., Int. Ed.*, 2025, **64**, e202505848.
- 166 O. Echeverria-Altuna, O. Ollo, I. Larraza, N. Gabilondo, I. Harismendy and A. Eceiza, *Polymer*, 2022, **263**, 125515.
- 167 Y. Su, S. Ma, B. Wang, X. Xu, H. Feng, K. Hu, W. Zhang, S. Zhou, G. Weng and J. Zhu, *React. Funct. Polym.*, 2023, **183**, 105496.
- 168 Y. Hu, Y. Tian, J. Cheng and J. Zhang, *ACS Sustainable Chem. Eng.*, 2020, **8**, 4158–4166.
- 169 T. Wang, H. Deng, N. Li, F. Xie, H. Shi, M. Wu and C. Zhang, *Green Chem.*, 2022, **24**, 8355–8366.
- 170 L. Zhou, S. Xiang, C. Wang, H. Zhang, K. Zhang and M. Chen, *Chem. Eng. J.*, 2024, **496**, 153901.
- 171 P. Zhao, J. Zhang, Y. Lou, J. Li, G. Han, S. Zeng, Y. Wang, Y. Liu and H. Yu, *ACS Mater. Lett.*, 2024, **6**, 3226–3237.
- 172 Z. Geng, A. Pang, T. Ding, X. Guo, R. Yang, Y. Luo and J. Zhai, *Macromolecules*, 2022, **55**, 8749–8756.
- 173 H. Wang, J. Huang, W. Liu, J. Huang, D. Yang, X. Qiu and J. Zhang, *Macromolecules*, 2022, **55**, 8629–8641.
- 174 W. Liu, C. Fang, S. Wang, J. Huang and X. Qiu, *Macromolecules*, 2019, **52**, 6474–6484.
- 175 X. Shi, S. Gao, C. Jin, D. Zhang, C. Lai, C. Wang, F. Chu, A. J. Ragauskas and M. Li, *Green Chem.*, 2023, **25**, 5907–5915.
- 176 Y. Huang, K. Jiang, Y. He, J. Hu, K. Dyer, S. Chen, E. Akinlabi, D. Zhang, X. Zhang, Y. Yu, W. Yu and B. B. Xu, *Adv. Mater.*, 2025, **37**, 2502266.

